POLITECNICO DI TORINO

MASTER's Degree in BIOMEDICAL ENGINEERING

MASTER's Degree Thesis

Synthesis and characterization of polymeric nanoparticles to target muscle cells

Supervisors

Prof. Valentina Alice CAUDA

Prof. Marta GUERRA

Candidate

Alice CAMBIASO

July 2025

Synthesis and characterization of polymeric nanoparticles to target muscle cells

Alice Cambiaso

Abstract

Duchenne muscular dystrophy (DMD) is a genetic disorder characterized by progressive degeneration of muscular tissue, caused by mutations in the dystrophin gene. It primarily affects males and leads to an average life expectancy of twenty years. Currently, there is no cure for DMD, but there are different treatments that attempt to improve quality of life and delay the disease's progression. The research is focusing on other strategies involving gene therapy as a potential cure for the disease. While these approaches are giving encouraging results, in the clinical trials they are not as effective as expected: the inflammation and associated defects in the muscles complicate their regeneration. This is connected to the fact that stem cells are exhausted. Previous studies have demonstrated that miR-106b negatively regulates myogenic factor 5, impairing the production of muscle progenitors. It has been observed that inhibiting miR-106b can promote muscle regeneration. A possible solution could be vectorizing anti-miR-106b sponges specifically to muscle stem cells. To accomplish this, polymers developed by Grup d'Enginyeria de Materials (GEMAT) could be used to synthesize nanoparticles (NPs) functionalized with targeting peptides. This study focuses on polymeric nanoparticles (NPs) functionalized with the AAVMYO peptide, a targeting ligand known for its high efficiency and specificity for muscle tissue. AAVMYO interacts with $\alpha_7\beta_1$ integrin, a laminin receptor overexpressed in DMD. We first corroborated its expression in C2C12 cell model using confocal immunofluorescence. Next, we focused on the uptake capacity of the NPs in different timing qualitatively and quantitatively. However, uptake levels for NPs with targeting peptides were not significantly higher than those without, suggesting limited targeting efficiency. To investigate further, we decided to conduct competition experiments between the peptide alone and our NPs and to verify, through confocal immunofluorescence, if the polymer with the peptides and the genetic material carried by the NPs colocalize. Our results indicate that the peptide's targeting ability is not functioning as expected probably because of poor surface exposure of the peptide. A potential strategy to improve the results could be to synthesize a OM-pBAE with Dibenzocyclooctyne (DBCO), in which the peptide will be attached to the lateral chains thanks to the click chemistry. While the findings of this study are promising, future research should focus on optimizing peptide presentation to enhance targeting efficiency.

ACKNOWLEDGMENTS

Agli in bocca al lupo e agli altri scongiuri che non si possono dire.

Table of Contents

List of Figures

List of Tables

List of Equations

Acronyms

DMD	Duchenne Muscular Dystrophy.
DGC	Dystrophin Glycoprotein Complex.
AAV	adeno-associated virus.
ASO	antisense oligonucleotide.
SCs	Satellite stem Cells.
miR	microRNAs.
NPs	Nanoparticles.
OM-pBAEs	oligo-modified poly beta esters.
GEMAT	Grup d'Enginyeria de Materials.
K	Lysine.
R	Arginine.
H	Histide.
RAFT	reversible addition fragmentation chain transfer.
P2	peptide 2.
P4	peptide 4.
PBS	Phosphate-buffered saline.
PFA	Paraformaldehyde.
DMSO	Dimethyl Sulfoxide.
DLS	Dynamic Light Scattering.
PDI	Polydispersity Index.

NTA	Nanoparticle tracking analysis.
DBCO	Dibenzocyclooctyne.
DMEM	Dulbecco's Modified Eagle Medium.
FBS	Fetal Bovine Serum.
HS	Horse Serum.
Cy5	Cyanine 5.
Cy3	Cyanine 3.
APC	Allophycocyanin.

Chapter 1

Introduction

1.1 Duchenne Muscular Dystrophy

Duchenne Muscular Dystrophy (DMD) is a X-linked genetic disorder. It was named after the French physician Duchenne de Boulogne, who wrote a clinical monograph about it in 1968, but its symptoms have been described since 1850 [1]. It is caused by mutations in the dystrophin gene that lead to an absence of functional dystrophin protein. Being an X-linked disorder (dystrophin gene is on X chromosomes), it affects mainly male newborns, nearly 1 in 5000 to 1 in 6000 [2]. As for females, if they inherit the mutation on one of their X chromosomes, they will only be carriers of the disease, since the healthy dystrophin gene on the other chromosome will provide enough functional dystrophin [3].
The dystrophin gene is one of the largest human gene having 79 exons, and frameshifting or nonsense mutations in it bring to have malfunctioning and unstable dystrophin [2][3]. Dystrophin is a 427 kDa cytoskeletal protein and it is widely expressed in skeletal, cardiac and smooth muscle cells. It resides at the cytoplasmatic side of the sarcolemma. Dystrophin has four main domains:

- an amino-terminal domain that binds with actin;
- a central rod domain, which contains 24 spectrin repeats, a cytoskeleton protein;
- a cysteine-rich domain;
- a carboxyl terminus, which connects the protein to the cell membrane.

The first domain mentioned is particularly important because it connects dystrophin to the subsarcolemmal actin network and to the contractile apparatus in skeletal muscle cells. Along with other proteins, including dystroglycan, sarcoglycans and sarcospan, it forms the Dystrophin Glycoprotein Complex (DGC) (**figure 1.1**). It is found in the cell membrane and connects intercellular cytoskeleton to extracellular matrix and it is supposed to have a central structural role acting as membrane stabilizer during muscle contraction to prevent damages induced by the contraction itself. It is hypothesized also to mediate cell signalling, as well as cell adhesion and mechanical force transduction [4].

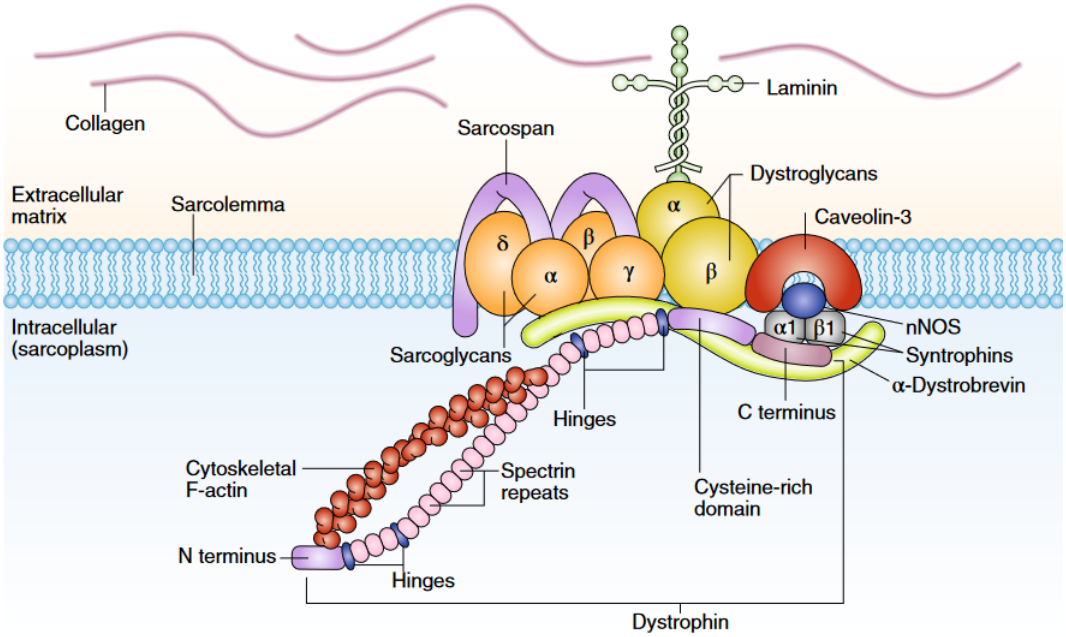

Figure 1.1: Schematic representation of dystrophin, a cytoskeletal protein found in the cytoplasmatic face of sarcolemma. Composed by four domain, together with different proteins, as dystropglycans, sarcoglycans and sarcospan among others, dystrophin forms the DGC. [5].

In pathological individuals, the results of having mutated dystrophin are a weakening of the connection between the sarcolemma and the cytoskeleton and the consequent damaging of muscle fibres during contraction. This leads to a chronic inflammation and the inhibition of muscle fibre regeneration. Hence, muscle tissue is replaced by fibrotic and adipose tissue, resulting in a progressive loss of muscle mass and a lowering of muscle quality [3].

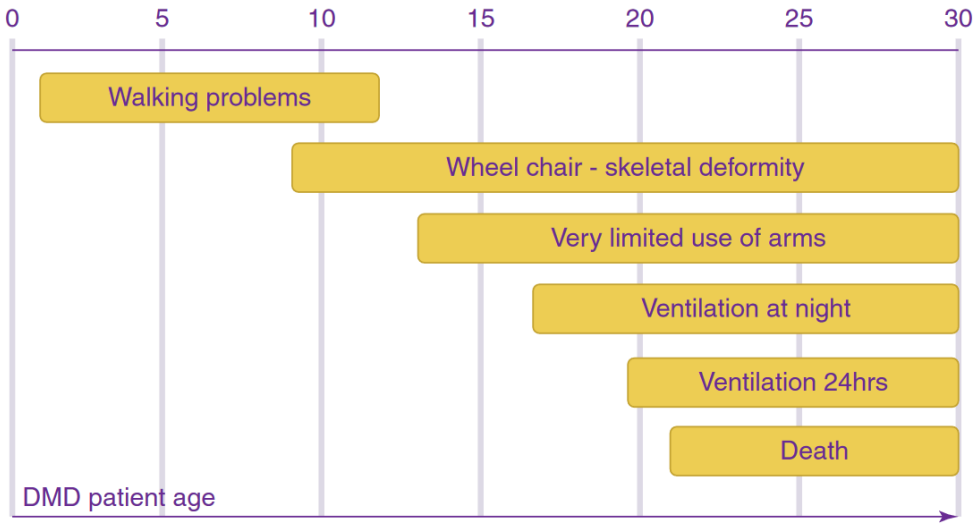

Figure 1.2: Schematic timeline of DMD symptoms progression [7].

Boys with DMD start presenting symptoms between 3 and 5 years of age. The first more common clues are gross motor delay, difficulties in rising from the ground or in walking and frequent falls. When they are 6 years old, there is a progressive downfall in muscle strength and untreated children have to use a wheelchair by 12 years. Growing up, they have to face cardiac problems, as dilated cardiomiopathy and arrhythmias, and respiratory issues, as chronic respiratory insufficiency. Additionally, orthopaedic complications as scoliosis are common if not treated. Patients around 20 years old will probably need assisted ventilation and about 40% of patients die of cardiac causes in their twenties, if not treated [6] (**Figure 1.2**).

1.2 Current treatments

At the moment DMD does not have a cure, but the current treatments can improve significantly the quality of life of people affected by this disease. It is necessary to take care of several aspects of patients' health (**Figure 1.3**). One element that contributes notably to enhance the quality of life are corticosteroids. They are used to improve respiratory function and muscle strength, prolonging ambulation by up three years and they reduce the risk of scoliosis. However, there are different side effects related to these pharmaceuticals, such as weight gain, worsening of bone health and also of behavioural issues [6]. This is not the only treatment that is usually done, because people affected by DMD are monitored for respiratory, cardiac and orthopaedic issues together with general check ups. Common standards of care for respiratory problems include the use of respiratory assist devices and non-invasive ventilation, while regarding the cardiac ones it is important to prevent cardiomyopathy utilizing angiotensin converting enzyme inhibitors, angiotensin receptor blockers and beta blockers. Therefore, some strategies and cure to enhance the quality of life have been developed, but they are not a definitive cure and they bring with themselves some side effect, as mentioned in the case of corticosteroids [3].

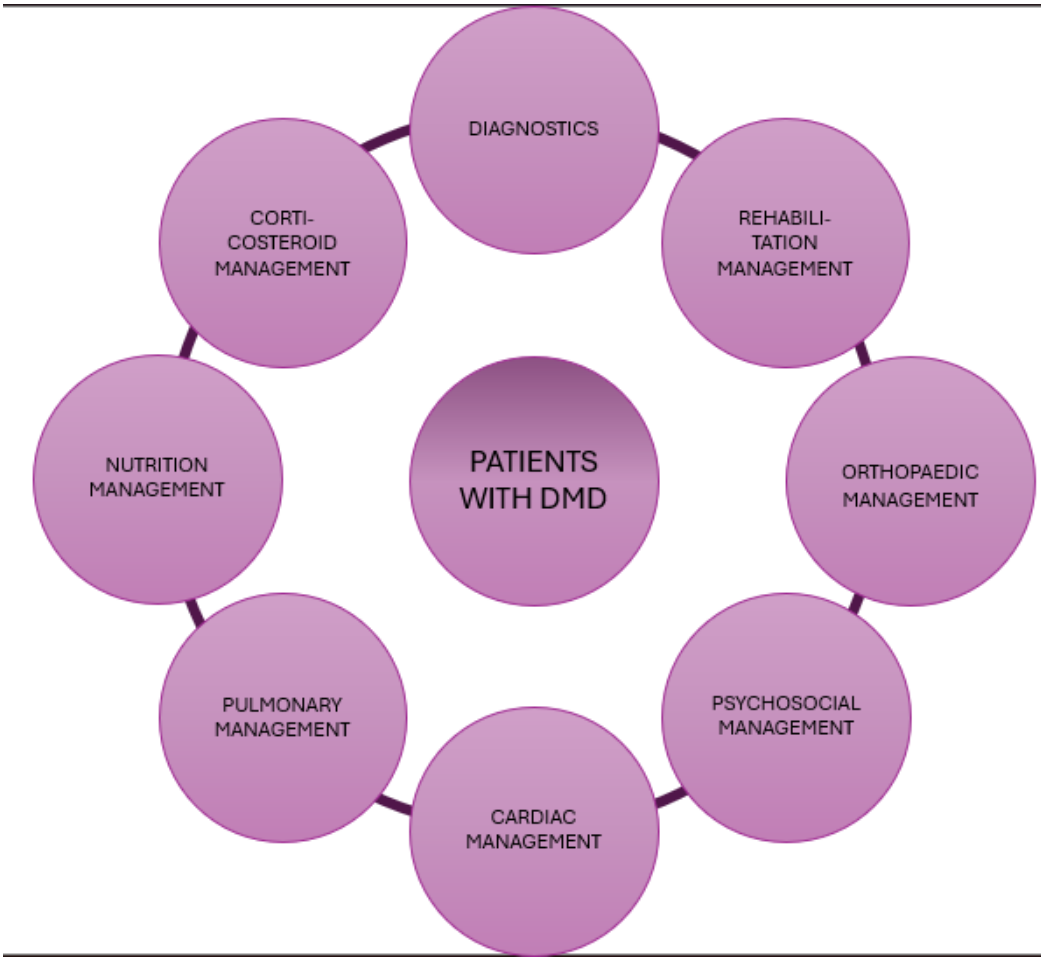

Figure 1.3: Taking care of patients with DMD requires an interdisciplinary management and it is crucial to coordinate every aspect to have enhanced results. The clinical treatments can range from pulmonary management to cardiac, nutrition, orthopaedic management and many more. All these treatment do not represent a cure, but they can improve the quality of life and extend life expectancy of patients.

1.3 Gene Therapy

Lately, the research has focused on gene therapy as a possible solution for DMD. Since the absence or shortage of functional dystrophin is what causes the physical issues in patients affected by DMD, the direct solution would be to replace the dystrophin gene with gene therapy. The target is to reach at least 10% of the dystrophin abundance in muscle seen in people without DMD mutations. As vector, the recombinant adeno-associated virus (AAV) represents a good candidate, as most serotypes could transduce skeletal muscle with high efficiency [3]. One problem about this strategy is the large size of the gene because the virus is only capable of packaging genomes and transgenes of limited size. For this reason, scientists have studied the sequence of the protein and its domains with the purpose of removing some coding sequences within the gene, maintaining at the same time the most protein functions as possible. Different variants of mini-/micro-dystrophins have been generated. Given the promising results with large animals, some human clinical trials are ongoing, as the ones by Sarepta Therapeutics and Pfizer. Each trial is using a slightly different mini-/micro-dystrophin construct delivered employing AAV [8].
Another strategy is exon skipping gene therapy. This approach aims to use antisense oligonucleotides (ASOs) to direct the cell's splicing machinery to ignore the mutated exon and the out-of-frame exons to restore the reading frame [5]. The result is a partially functional dystrophin. An important aspect to notice is that this treatment is mutation-dependant and the specific exon-skipping strategies are applicable only to a limited group of DMD patients. However, the ensemble of exon skipping strategies, with various medicinal products, can possibly treat around 60% of DMD patients.
Gene therapies in general are very promising, but the results of the clinical trials are not as good as expected as there are, like in most new strategies, different obstacles and disadvantages to overcome. One among the others is the fact that mini-/micro-dystrophins are used instead of the full protein. Moreover, due to the immune response, it is important to consider the potential loss of gene therapy effectiveness over time. Another fundamental aspect is that the absence of dystrophin results also in chronic inflammation with the consequent replacement of muscle with fibroadipose tissue: there is a lack of proper muscle regeneration that help the loss of muscle tissue and inhibit the success of gene therapies [9].

1.4 Muscle regeneration in DMD

As just mentioned in the prior section, the defects in muscle regeneration contribute to the progressive lost of muscle mass and the cause can be found in the decreased capability of muscle stem cells to generate new cells. This ability is peculiar to the skeletal muscle, which is one of the few tissue to have it. This is possible thanks to the satellite stem cells (SCs) that are between the basal lamina and sarcolemma of myofibers. They are usually mitotically quiescent, but after an injury or an intensified contractile activity, where there is inflammation, they activate, proliferate and enter into the myogenic program via PAX7 downregulation and the activation of myogenic regulatory factors as MYF5, MYOD1, MYOG and MYF6. PAX7 is a gene that encodes the transcription factor Pax-7, which plays a key role in myogenesis through regulation of muscle precursor cells proliferation. Activated SCs go through symmetric or asymmetric divisions:

- symmetric division helps to restore the stem cell pool;
- asymmetric division generates both stem cells and differentiated ones.

The first myogenic regulatory factor to be expressed is MYF5 and its upregulation, followed by the one of Myod1, is needed for myogenic determination. Activated SCs go where the injury is and form new myofibers or fuse with ones already present. All these processes are guided by the regulated expression of different factors and different kind of cells are involved, as vascular, inflammatory and mesenchymal cells. Other elements that play an essential role in regulating muscle regeneration are microRNAs (miR)[9].

1.5 miR-106b

miRNA are small non-coding RNA needed for the post-transcriptional control of gene expression. Recent studies have suggested that in the case of muscular dystrophies, some of the miRNAs involved in muscle regeneration are altered and these variations are connected directly to the loss of regeneration capability.
In this project, we focus on miR-106b. Its role has been studied and it has been demonstrated that miR-106b has a key role in regulating SCs behaviour, since it is a quiescence modulator for them. To have a physiological muscle regeneration its downregulation is needed. In our work it is particularly interesting because it has also been seen that in dystrophic mice and humans, miR-106b increase in the muscle SCs. If intramuscular injection of miR-106b inhibitory molecules (anti-miRNA) are carried out in injured dystrophic mice, muscle regeneration is improved. Anti-miRNA are chemically modified single-stranded RNA molecules. They are designed to specifically bind to and inhibit endogenous miR molecules by down-regulation of miR activity [10][11].
Knowing this and that gene therapy looses efficiency due to the defects in muscle regeneration, an enhanced strategy for DMD would be to combine gene therapy and the inhibition of miR-106b to improve muscle regeneration. Our work focuses on designing and vectorizing anti-miRNA-106b specifically directed to muscle SCs. The need of a vector to deliver it, besides the specific targeting, is given by the fact that, due to the lipophilic nature of cell membranes, genetic material cannot cross them [12].
The idea is to use synthetic polymeric nanoparticles (NPs), synthesized with oligo-modified poly-beta esters (OM-pBAEs) developed by Grup d'Enginyeria de Materials (GEMAT).

1.6 Nanoparticles

In the last decades, nanotechnology collected interest in the scientific community for its many potential uses across various field of application. The term nanotechnology indicates the application of scientific and technological knowledge to control and manipulate materials at the nanoscale. NPs, as defined by the British Standards Institution, are particles having a nanometric size of around 100 nm in all directions (x,y,z)[13], [14], [15]. In the healthcare field, NPs can be seen as delivery vehicles for drugs, but also for genetic material, as in the case of this project. They are gaining more importance in the research thanks to their ability to possibly improve the performance of what they are delivering in term of body entrance, targeting, flexible release conditions and in reducing side effects [12].

1.6.1 History of NPs

Nanomaterials had been produced and used long before recent times, but the start for modern nanotechnology takes back to 1857 with Michael Faraday, who reported the synthesis of gold colloidal particles (**Figure 1.4**). He studied also optical properties, but the reasons for those were explained only later by Mie (1908). In the 1940s, SiO2 NPs were fabricated, but it was the publication of Richard P. Feynman ("There is plenty of room at the bottom") that opened the new field of nanotechnology [15], [16].

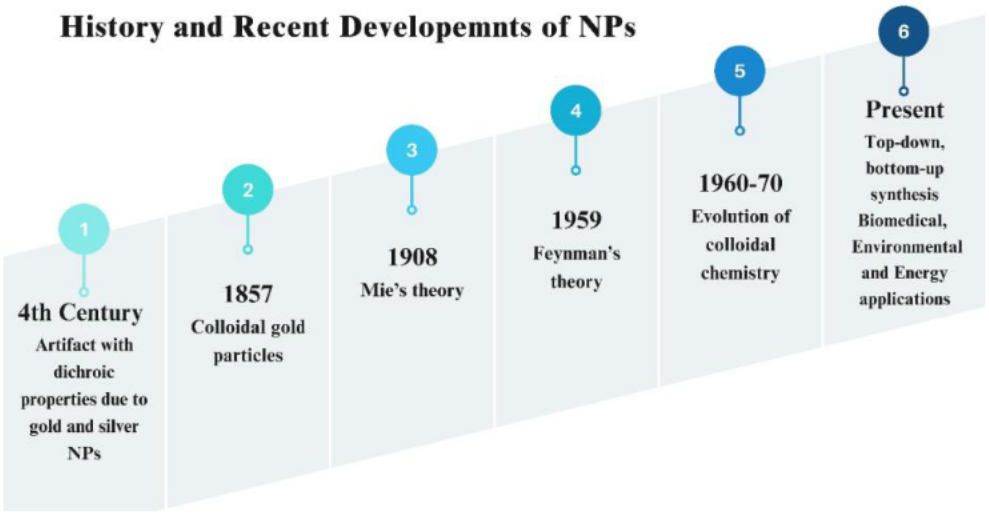

Figure 1.4: Some of the most important highlights of the modern history of NPs and nanomaterials. From 1857 with the colloidal gold NPs to the present, with different synthesis techniques and application.[14]

1.6.2 Classification of NPs

NPs can be classified according to their structure (**Figure 1.5**):

- nanocapsules, solid NPs with a shell surrounding the core, a reservoir space;
- nanospheres, homogeneous matrices whose entire volume is full.

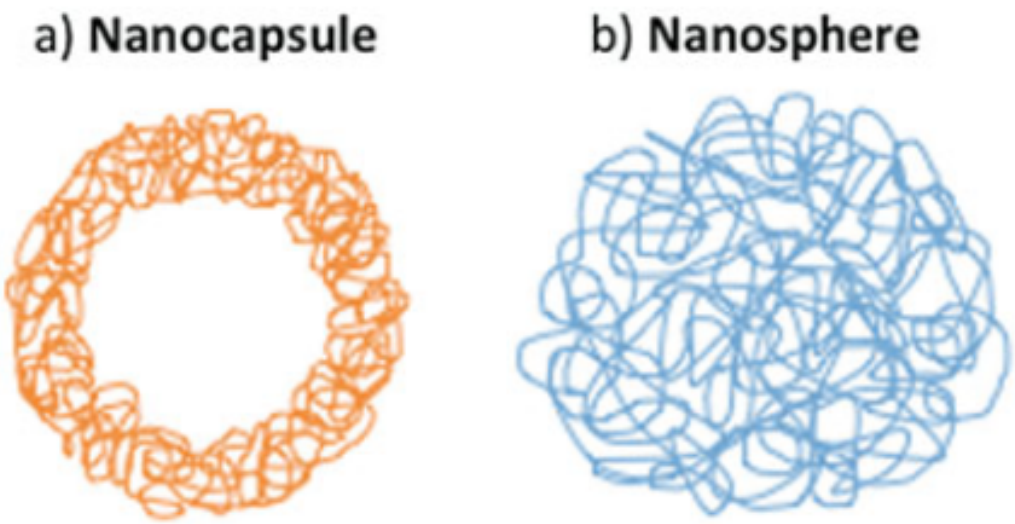

Figure 1.5: Schematic representation of a nanocapsule and a nanosphere [12].

NPs can also be classified for the material from which they are composed. We can divide them in three main groups, organic, inorganic and Carbon-based NPs, that can be divided in subgroups themselves as shown in the following scheme (**Figure 1.6**).

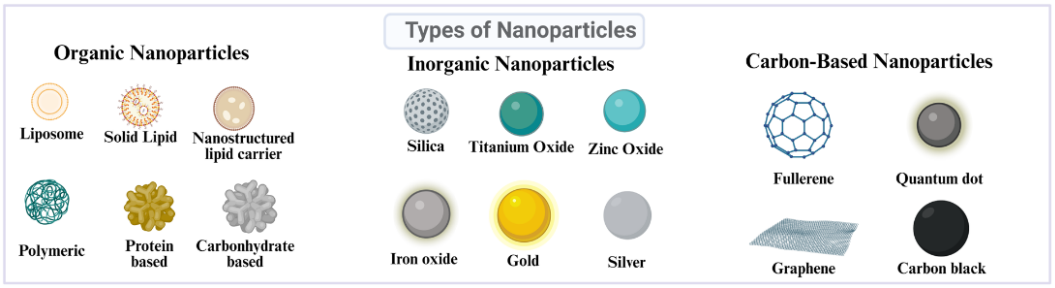

Figure 1.6: Classification of NPs according to the materials they are composed by (adapted from [17]).

Our focus will be on polymeric NPs, that in the last decades have gained an important place in the therapeutic and diagnostic research given their properties. Polymers, in fact, are composed of repeated monomers and there are many features that can change, as their structure or their size. They can be easily functionalized and their production can be affordable and scalable. Polymeric NPs can be synthesized starting from natural or synthetic polymers, both have their advantages and disadvantages. Natural polymer vectors have shown enhanced cell transfection and

cell viability compared to the synthetic ones. However, they are more expensive to produce in large-scale quantities and there is also the possibility to provoke immune responses. Synthetic polymer vectors can show similar properties compared to the natural ones, but without the mentioned downsides [18]. They also are more stable. In our project, the NPs are composed by the synthetic polymers OM-pBAEs, as already mentioned [17].

1.7 Polymers OM-pBAE

pBAEs are a class of biocompatible and biodegradable polymers. They are composed by ester bonds, which are degradable in physiological conditions [19]. In 2000 Lynn et al. described for the first time pBAEs as nucleic acid cationic carriers of second generation [20] and then in the last twenty years the research has developed and modified them reaching some important milestone as shown in **Figure 1.7**, understanding their importance in possible immune therapeutic applications. In particular, in 2014 Segovia et al. [18] modified the ends of pBAEs with amine-rich oligopeptides obtaining OM-pBAEs.

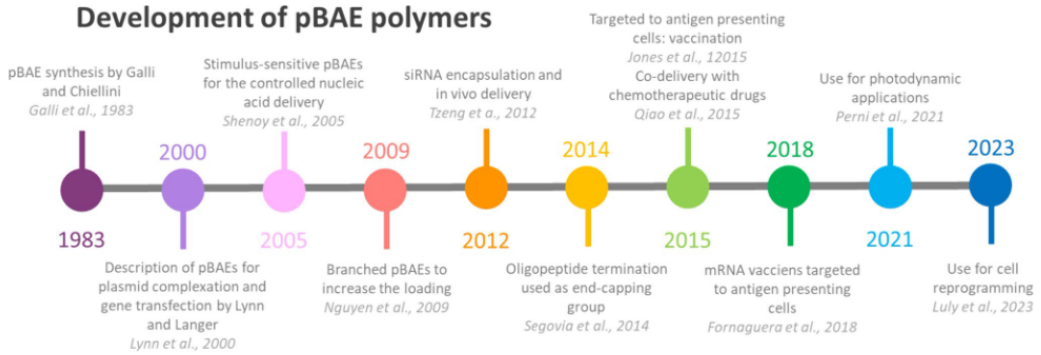

Figure 1.7: Highlights of PBAEs development, in particular for immune therapeutic applications [21].

The question now is why this family of polymers is the right choice for our project, besides the already mentioned general advantages of synthetic polymers.
Firstly, generally the encapsulation of genetic material, which is characterized by negative charge, happens due to electrostatic interactions, so it is necessary to have a cationic vector. pBAEs are a better choice comparing to other carriers due to their pH-dependent charge, which facilitate binding to negatively charged genetic material. The electrostatic interactions also bring to have NPs with a minimal energy input, as manual pipetting and the entrapment efficiency is high: pBAEs in contact with polynucleotides condense into polyplexes. This is important also to protect the cargo during the transportation to the targetted cells. Furthermore, pBAEs are biocompatible and biodegradable. Another significant benefit is that their synthesis is rapid and simple: they are synthesized by Michael addition between diacrylates and primary amines. This also allows to bring in structural diversity adding several functionalities. pBAEs building blocks contain hexil monomers (C6) that give a certain level of hydrophobicity to the polymer, important to permit to the NPs to be freeze-dried and re-dispersed keeping their characteristics, which is a very important feature.

As already mentioned, in 2014 Segovia et al. functionalized the pBAEs polymers with short cationic oligopeptides, such as lysine (K), arginine (R) and histidine (H) (**Figure 1.8**), obtaining OM-pBAEs (**Figure 1.9**).

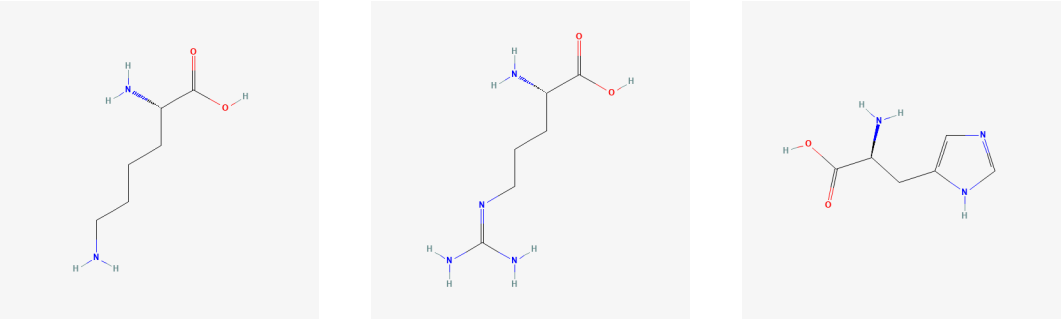

(A) (B) (C)

Figure 1.8: Chemical structure of lysine (A) [22], arginine (B) [23], and histidine (C) [24].

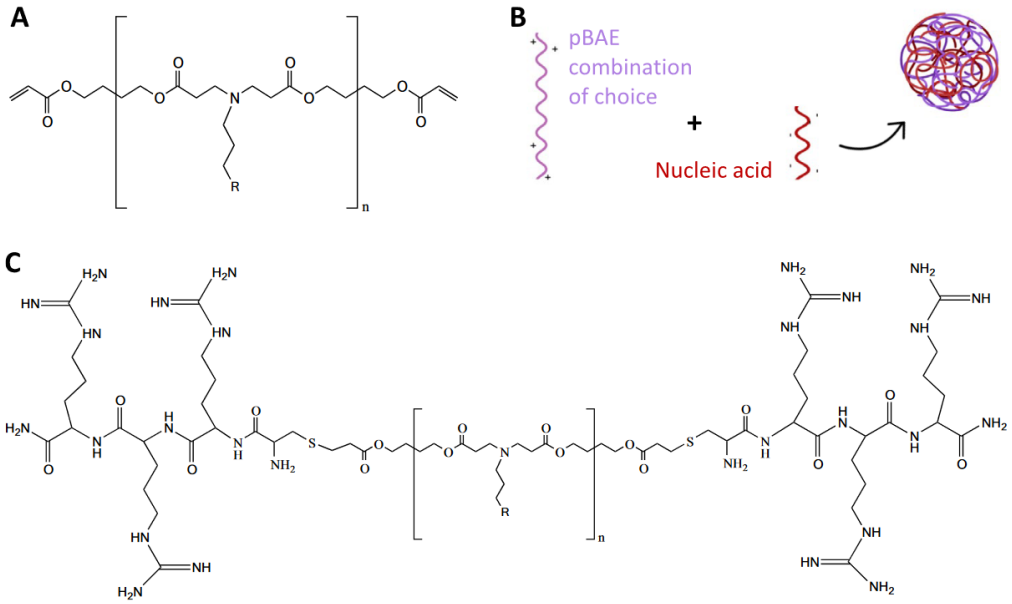

Figure 1.9: Schematic representation of pBAEs NPs composition and formation. **A**: Chemical structure of pBAE polymer backbone, including the end-oligopeptide modification, with n=6-8 repetitions and R= lateral chain functionalization. **B**:Formation of NPs thanks to the electrostatic interaction between the cationic polymer and the anionic nucleic acids. **C**: Chemical structure of OM-pBAE [21].

They are synthesized modifying acrylate-terminated pBAEs using thiol-ene chemistry. In general, they enhance the ability to compact nucleic acids due to electrostatic interactions, cellular internalization and nucleic acid transfection. The downside is that cationic peptides lead to a higher transfection promiscuity and therefore a low selectivity. This is still a consequence of their positive charge: cell membranes are negatively charged so they easily interact with the positive pBAEs NPs.
More specifically, K-modified pBAEs and R-modified pBAEs have been seen to achieve enhanced transfection efficiency, while H-modified pBAEs have demonstrated a better buffering capacity, needed for the endosomal escape. As it is important that the NPs enter the cell, it is as well its exit. H has the highest buffering capacity due to the lower pK_a of the imidazole ring, while R and K have a higher pK_a. H mediates the proton sponge effect, which is a phenomenon that facilitates endosomal escape.
Despite the individual properties of the OM-pBAEs, it has been observed that when the K- and R-modified pBAEs were formulated in combination with H-modified pBAEs, the transfection capacity further increased. In this project, in fact, we used a mixture of polymers with H and K [12][18][19][25][26][27].

1.7.1 Zwitterionic polymer

In this project, beside using the OM-pBAEs described, we synthesized our NPs using also a zwitterionic polymer developed by GEMAT group. Starting from OM-PBAE, the side chains were chemically modified to copolymerize zwitterionic monomers. They were synthesized through reversible addition fragmentation chain transfer (RAFT) living polymerization of methacrylate sulfobetaine monomers on the side chain of pBAE backbone (**Figure 1.10**). After this step, K oligopeptide was added modifying the acrylate ends of the PBAE through Michael addition reaction. The resulting graft polymer allows polyplex assembly as the cationic block can interact electrostatically with the genetic material. The zwitterionic graft gives to the polymer antifouling properties, leading to a reduction of the adsorption of proteins on the surface of NPs and preventing complement system cascade activation. This properties are very important, especially for applications that necessitate repeated or long-term administration. Another interesting characteristic is the lower Z-potential of the NPs formed with this polymer, that should slightly lower the transfection rate. In this project we want to target specifically muscle cells thanks to specific peptides, so if the NPs are not entering the cells so easily only for their positive charge, they could do so mainly for the specific interaction between the peptides and their target. Also in this case, the best strategy seems to synthesize NPs with a mixture of H-modified PBAEs and zwitterionic polymer capped with K [28].

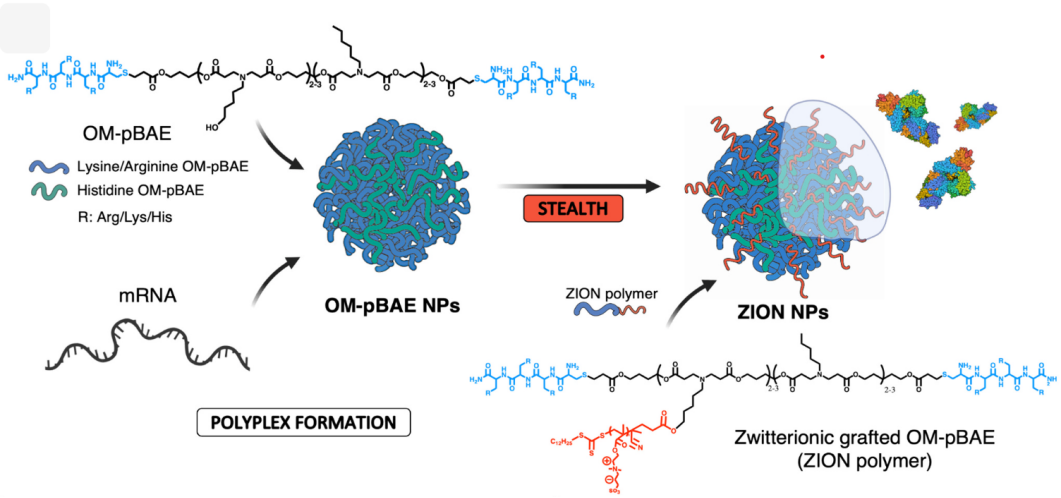

Figure 1.10: OM-PBAE and zwitterionic NPs preparation. In this example the genetic material shown is mRNA, but it can also be done with other genetic materials, as PGFP in the case of this project [28].

1.8 Targeting peptides

As indicated in the prior sections, our aim is to target muscle cells specifically. In order to accomplish this, we added to the NPs a targeting peptide, AAVMYO. It is a peptide-displaying AAV9 mutant. AAV are, in fact, the basis for several commercial gene therapy products and for gene transfer vectors. AAVMYO showed great potential for muscle gene therapy since it exhibited higher efficiency and specificity for the musculature including skeletal muscle, heart and diaphragm from peripheral delivery [29]. This peptide binds to the $\alpha_7\beta_1$ integrin which is a laminin receptor located on the surface of skeletal myoblasts and myofibers. This integrin is a excellent target because it seems related to several muscle disease: in DMD it is possible to see a higher expression of $\alpha_7\beta_1$-mediated linkage of the extracellular matrix. This could compensate for the absence of the dystrophin-mediated linkage. We are going to use two different targeting peptide based on the AAVMYO structure, that we are going to call peptide 2 (P2) and peptide 4 (P4).

1.9 Objectives

The aim of this master thesis is to establish the capacity to specifically transfect to muscle cells of our NPs, composed by OM-pBAEs and zwitterionic PBAEs polymers, combined with targeting peptides. To reach this main purpose, there were several secondary objectives to achieve:

- confirm the presence of the integrin $\alpha_7\beta_1$, which is te target of the chosen peptide through confocal analysis;
- synthesis and characterization of PBAEs NPs;
- study the uptake capacity of the NPs in different timing;
- verify the specific targeting of the AAVMYO through competition experiments
- verify the colocalization of the polymers with the peptides and the genetic material through confocal analysis;
- try to improve peptide's exposition using OM-pBAE with DBCO.

Chapter 2

Material and Methods

2.1 Localization of integrins $\alpha_7\beta_1$ and Desmin

Confocal microscope was used to visualize integrins $\alpha_7\beta_1$ and Desmin both with non differentiated and differentiated cells. To prepare the samples we used 24-plate wells, where we inserted cover glasses with a 14 mm diameter (Superior Marienfeld). They were exposed under UV light for 10 to 20 minutes to sterilize them. To seed non differentiated cells, 400 μL/well of Bovine Gelatin (2% in water, Sigma-Aldrich®) 0,1% in Phosphate-buffered saline (PBS) were put in each well to enhance cells adhesion. After 3h at 37°C, gelatin was removed and $7 * 10^4$ cells/well were seeded and left incubating for 24h. As for differentiated cells, we followed the procedure described in the **section 2.4**. Once the cells were ready, the culture medium was removed and the wells were washed with PBS. 250 μL/well of Paraformaldehyde (PFA) 4% were added to fixate the cells. The plate was kept at 25°C covered in aluminium foils. After 30 minutes, PFA was removed and 250 μL/well of Tween 20 (Sigma-Aldrich®) 0,1% in PBS were added to permeabilize the samples. After 30 minutes it was removed and milk powder 5% in PBS was added as blocking solution. Once waited for 1 hour, always at room temperature, the milk powder was removed. The antibody used were the following (**Table 2.1**):

Antibodies	
Primary antibody for α_7	ITGA7 Polyclonal Antibody, Invitrogen
Primary antibody for β_1	CD29 (Integrin beta 1) Monoclonal Antibody (TS2/16), eBioscience™
Primary antibody for Desmin	Desmin Polyclonal antibody, Proteintech®
Secondary antibody for α_7 and Desmin	Goat anti-Rabbit IgG (H+L) Cross-Adsorbed Secondary Antibody, Alexa Fluor™ 568, Invitrogen
Secondary antibody for β_1	Goat anti-Mouse IgG (H+L) Cross-Adsorbed Secondary Antibody, Alexa Fluor™ 700, Invitrogen

Table 2.1: Antibodies used for the analysis of the integrins α_7, β_1 and Desmin.

Primary antibodies were diluted in milk powder 5% in PBS with a ratio of 1:100 and secondary antibody with 1:500. 10 μL of primary antibody were placed on a piece of Parafilm. The cover glasses were then laid on the drop, with the side covered by the cells facing down. The samples were left incubating in a dark box in a humid environment for one night at 4°C. Subsequently, the same procedure was repeated with the secondary antibody, but with a incubation of 1 hour at 25°C. After, this was repeated also with a drop of DAPI, but we waited only for 20 minutes. A wash with PBS was done. The cover glasses were placed, always with the side with cells facing down, on the rectangular cover slips, where previously 10 μL of Fluoromount™ Aqueous Mounting Medium were added. The samples can be stored at 4°C and they were analysed with Confocal microscope (Leica DMi8). The images obtained were processed using ImageJ software.

2.2 Polymeric Nanoparticles

2.2.1 Synthesis of OM-pBAEs NPs

Polymeric NPs were synthesized following the protocol developed by the GEMAT group. Acetate buffer was prepared from NaAc stock solution 3M (Sigma-Aldrich, USA) and diluted in MilliQ water to reach a concentration of 12.5 mM. Its pH was adjusted to 5.2 and then it was filtered. This buffer could be stored at 4°C for a maximum period of three months. The polymers used, OM-pBAE (C6) and the zwitterionic (ZW) polymer, were synthesized in-house and already capped with different peptides, as shown in the following table (**Table 2.2**):

Polymers	Peptides used for capping	Resulting Polymers
C6	Lysine (K)	C6-K
	Histide(H)	C6-H
	Peptide 2	C6-P2
	Peptide 4	C6-P4
ZW	Lysine (K)	ZW-K

Table 2.2: Table of polymers capped with peptides used in this project.

The resulting polymers were diluted in Dimethyl Sulfoxide (DMSO, Sigma-Aldrich, USA) to obtain a concentration of 100 mg/mL and stored at -25°C. The genetic material used was PGFP (Gigaprep from E.Coli DH5α). It was stored at -25°C with a concentration of 1 mg/mL.
Polymers were thawed and vortexed. They were then diluted in the acetate buffer to reach required concentrations. Regarding NPs synthesized with C6, this was 12.5 mg/mL, as a consequence of the NP/polymer ratio used, which was 25:1. Instead, for the zwitterionic one, the desired concentration was 17.5 mg/mL, as the NP/polymer ratio used was 35:1. Similarly, PGFP was added to NaAc buffer to reach a concentration of 0.5 mg/mL.
The genetic material was added to the polymers solution with a 1:1 ratio and pipetted at least for 30 seconds, avoiding bubbles. After 20 minutes of incubation at room temperature, an equal volume of MilliQ water was added to the mixture. Then, the same volume of MilliQ water was added again. As a result of these two dilutions, the final concentration of PGFP was 0.083 mg/mL. NPs can be stored for a short time at 4°C.
In this project, we chose the composition of the NPs based on previous studies. The different percentages utilized are shown in the following table (**Table 2.3**).

NPs	**C6-K**	**C6-H**	**ZW-K**	**C6-P2**	**C6-P4**
KH	60%	40%	0%	0%	0%
KH_{54}	54%	36%	0%	0%	0%
KHp2	54%	36%	0%	10%	0%
KHp4	54%	36%	0%	0%	10%
ZWH	0%	40%	60%	0%	0%
ZWHp2	0%	30%	60%	10%	0%
ZWHp4	0%	30%	60%	0%	10%

Table 2.3: Composition of NPs synthesized and used in this project.

2.2.2 Dynamic light scattering (DLS) and Z-potential

NPs were analysed using a Zetasizer Nano ZS with the Zetasizer Software (Malvern Instruments, Worcestershire, UK). We characterized their hydrodynamic diameter, polydispersity index (PDI) and surface charge (Z-potential). For the first two, it was necessary to insert at least 30 μL of NP in a DLS cuvette. Regarding the Z-potential, 30 μL of NP were diluted in 900 μL of MilliQ water. The solution was then moved to a Disposable Capillary Cell (DTS1060, Molvern Instruments, Worcestershire, UK).

2.2.3 Nanoparticle tracking analysis (NTA)

A further analysis was done with Nanoparticle Tracking Analysis Nanosight NS300 (Malvern Panalytics, United Kingdom) to obtain the size distribution of the NPs. 10 μL of the sample were diluted in 1 mL of MilliQ water (1:100) and then pumped in the machine using a syringe.

2.3 Synthesis of OM-pBAEs-DBCO NPs

OM-pBAEs-DBCO NPs were synthesized following the same procedure described in the previous section, with the addition of Dibenzocyclooctyne-amine (DBCO-NH_2) in the polymers. To do so, we used a OM-pBAEs polymer C6 that was synthesized in-house, contained already the DBCO-NH_2 and was also capped with K (C6-DBCO-K). As for the polymeric composition of the NPs, we chose as template KH, in which there is 40% of C6-H and 60% of C6-K, as indicated in the **Table 2.3**. The quantity of C6-H was maintained the same, whereas C6-K was replaced by a part of the same C6-K and a part of C6-DBCO-K. We analysed different percentages of these last two components, as shown in the **Table 2.4**:

NPs	**C6-K**	**C6-DBCO-K**
$DBCO_{1\%}$	99%	1%
$DBCO_{10\%}$	90%	10%
$DBCO_{50\%}$	50%	50%
$DBCO_{100\%}$	0%	100%

Table 2.4: Different percentages of C6-K and C6-DBCO-K used for synthesizing OM-pBAEs-DBCO NPs. The percentages refer as total to the quantity of the polymer C6-K that would be in the normal KH, which corresponds to 60% of the total polymeric composition. The remaining part is C6-H.

Once synthesized, their size, PDI and Z-potential were analysed using the DLS and the NTA, as explained in the previous sections. Subsequently, we added to the NPs a modified P2 containing an azide group, which would bind with the DBCO by click chemistry. The incubation time was 30 minutes and the samples were kept at room temperature.

2.4 Cell Culture

In this project C2C12, a myoblast cell line, was used. They were maintained in Dulbecco's Modified Eagle Medium (DMEM) supplemented with 10% (v/v) Fetal Bovine Serum (FBS, Biowest®, France), 1% (v/v) L-Glutamine (Sigma-Aldrich®, USA) and 1% (v/v) Penicillin/Streptomycin (Biowest®, France). The cells were cultured at 37°C under a 5% CO2/95% air atmosphere. They were passaged before arrive to a confluent status, normally after 3 days of incubation.

2.4.1 Cell thawing and freezing

Cells were kept stored at -150°C in cryovials with a concentration of 10^6 cells/mL. To thaw cells, they were submerged in a 37°C bath for some seconds, then they were transferred into a Falcon tube. 5 mL of DMEM 10% FBS were added and it was centrifuged for 5 minutes at 1500 rpm. The supernatant was aspired and the pellet was resuspended in 1 mL of DMEM 10% FBS. It was then moved into a Petri dish with additional DMEM.
To freeze cells, once counted, they were resuspended in a freezing solution to have a density of 10^6 cells/mL and 1 mL was placed per cryovials. The freezing solution was half composed by DMEM 10% FBS (v/v) and half by FBS with 20% (v/v) of DMSO. Cells were stored for 24 hours in a isopropanol freezing container at -80°C, to be moved thereafter in a -150°C freezer.

2.5 Differentiation of C2C12 cell line

C2C12 can differentiate rapidly, forming contractile myotubes and characteristic muscle proteins. When they differentiate, they have the typical elongated shape of myotubes [30]. This process was effectuated in a 96 or 24-well plate, depending on the experiment to conduct. The wells were pretreated with bovine type I of collagen at a concentration of 100 μg/mL (80 μL/well for the 96-well plate and 400 μL/well for the 24-well plate). The collagen was diluted in Phosphate-buffered saline (PBS) as the stock concentration was 10 mg/mL. The plate was then incubated at 4°C overnight. Thereafter, collagen was aspirated and, in the case of the 96-well plate, 15000 cells/well were seeded. Instead, for the 24-well plate, 10^5 cells/well were seeded. After 24 hours of incubation at 37°C, the culture media was changed with 180 μL (for 96-well plate) or 600 μL (for the 24 well-plate) of DMEM supplemented with 2% (v/v) Horse Serum (HS), 1% (v/v) L-Glutamine and 1% (v/v) Penicillin / Streptomycin. The plate was left incubated for 4 days, after which differentiated cells were ready.

2.6 Labelling PGFP

In order to have detectable fluorescence of NPs, we decided to label PGFP with Cyanine 5 (Cy5, Lumiprobe, USA) following the protocol used by the GEMAT group. 0.5 mg of Cy5 were added to 5 mL of DMSO. 30 μL of PGFP (1 mg/mL) were mixed with 100 μL of Cy5 (10 mg/mL): the ratio has to be 10:3 (Cy5: PGFP). Cy5 was firstly diluted in DMSO to obtain the required concentration. The solution was stirred for 2 hours at room temperature with a magnet bar and a foil of aluminium to protect the mixture from light. It was then added a volume of 13 μL of NaCl (5M) and 286 μL of cold ethanol 100% (0.1 and the double of the volume of the solution respectively). Ethanol was left previously in the -20°C freezer overnight. Subsequently, the solution was centrifuged at 14000 rpm for 15 minutes at 4°C to obtain a pellet. This was washed with room temperature ethanol 70%. If necessary, the centrifuge and the wash could be repeated. We let the pellet air dry for 5-10 minutes and then we resuspended it in 15 μL of MilliQ water (0.5 of the volume of PGFP used).

2.7 Labelling of C6-pBAE

We followed the protocol used by GEMAT group to label the polymers used in the NPs with Cyanine 3 (Cy3, Lumiprobe, USA). C6-H had already being labelled with Cy3, so we focused on the pBAEs with the targeting peptides 2 and 4. 0.5 mg of Cy3 were added to 5 mL of DMSO. 30 μL of C6-P2 (100 mg/mL) were placed in an Eppendorf of 1 mL. 3.5 μL of triethylamine, 234 μL of DMSO and 50 μL of Cy3 were added. The solution was stirred for 24 hours, covered by aluminium foils. The solution was then added drop wise into a diethyl ether/acetone (7/3) mixture. Once vortexed, it was centrifuged at 4000 rpm for 10 minutes. The solvent was removed and this washes were repeated twice. The pellet obtained was vacuum dried for 24 hour and ultimately DMSO was added to have a concentration of 100 mg/mL. The same procedure was followed with C6-P4.

2.8 DNA uptake

Cells were seeded the day before in a 96-well plate with a concentration of 8000 cells/well if the uptake was to be conducted with non-differentiated C2C12. When the experiment was done with differentiated ones, cells were seeded following the differentiation protocol. NPs were synthesized carrying 1% of PGFP labelled with Cy5 and 99% of regular PGFP. The required amount of PGFP was 0.3 μg/well, so to determine the volume of NP needed, this calculation (**Equation 2.1**) was done:

$$V_{NPs} = N_{wells} * 0.3 \frac{\mu g}{well} * \frac{1}{0.083 \frac{mg}{mL}} \tag{2.1}$$

Equation 2.1: Equation to calculate V_{NPs}.

where V_{NPs} is the NPs volume needed, N_{wells} is the number of well that we want to do the uptake with and 0.083 $\frac{mg}{mL}$ is the concentration of PGFP in the NPs, as already indicated in **section 2.2.1**. The volume of NPs needed was then added to DMEM to reach 100 μL in each well.
The culture medium was replaced by the solution of NPs and DMEM. The negative control was given by using only DMEM, while the positive ones were the wells with NPs without the targeting peptides. The plate was incubated for different time (2, 4, 6 and 8 hours and overnight) to study the uptake of PGFP. The uptake was then stopped and the wells were analysed by flow cytometry.

2.9 Competition experiments

Cells were seeded as dictated by the DNA uptake protocol and NPs were also synthesized analogously. Firstly, we incubated the cells with peptide 2. As incubation times, we tried thirty minutes and one hour. To calculate the quantity of peptide needed, starting from the NPs synthesis protocol, we determined the amount of C6-P2 contained in a 45 μL NP. Knowing the molar ratio between the polymer and the peptide, we calculated the mass of peptide 2 contained in the volume of NPs in a well. The values change with the zwitterionic NPs, since the concentration of the polymer is higher, as explained in **section 2.2**. P2 was diluted in water at 1 mg/mL. We incubated cells with the calculated amount of P2 and also with the double. As control, we simultaneously did a normal uptake. We mixed P2 with enough DMEM to reach 50 μL in each well. After the established time, we incubated the NPs, as explained in the DNA uptake protocol, but using half of the DMEM volume, since it had already been added with the peptide.

2.10 Flow Cytometry

Uptake and competition experiment were analysed by flow cytometry. To do so the cell media was removed and the wells were washed with PBS to remove any trace of DMEM left. 25 μL/well (when using 96-well plate) of trypsin were added. It followed an incubation of 5 minutes at 37 ° C to detach the cells. After this, without removing the trypsin, 80 μL/well of a fixing solution were added. This was made by one part of para-formaldehyde (PFA, Sigma-Aldrich®, USA) 4% in PBS and two parts of DMEM 10% FBS. Cells were ready to be analysed by the ACEA Biosciences (now Agilent, USA) NovoCyte Flow Cytometry system. The machine was set to aspirate 90 μL of well volume out of the 95 μL totals and the Allophycocyanin (APC) filter was used to detect Cy5.

2.11 Localization of NPs

NPs were prepared with PGFP labelled with Cy5. To see also the polymers, we labelled also the peptides capped to the polymers used for the NPs, as described in **section 2.6**. In these NPs we had both PGFP and one polymer labelled, so we needed to have similar amount of Cy5 and Cy3. Since the concentration of Cy5 in PGFP was really low, we decided to increase at 10% the PGFP labelled in the NPs. Thanks to the calibration curve, we could calculate the quantity of Cy5 in one NP of 45 μL. From this, we could determine the percentage of labelled polymer that needed to be in the NPs to have a corresponding quantity of Cy3. To achieve our purposes, we prepared NPs where C6-H was labelled or where C6-P2 or C6-P4 were labelled.

As for the cells, after the fixing and the blocking processes, they were stained with DAPI, following the same procedure described in **section 2.1**. The cover glasses were then placed on rectangular cover slips with a drop of Aqueous Mounting Medium.

Chapter 3

Result and Discussion

3.1 Analysis of integrin $\alpha_7\beta_1$ and Desmin

Firstly, it was fundamental for our research to corroborate the expression of the integrin α_7/β_1 in C2C12 cell model, which increases and changes the location into the membrane in differentiated cells, according to previous studies [31]. An immunofluorescence analysis was performed on non-differentiated cells and 5-days differentiated ones (**figure 3.1**).

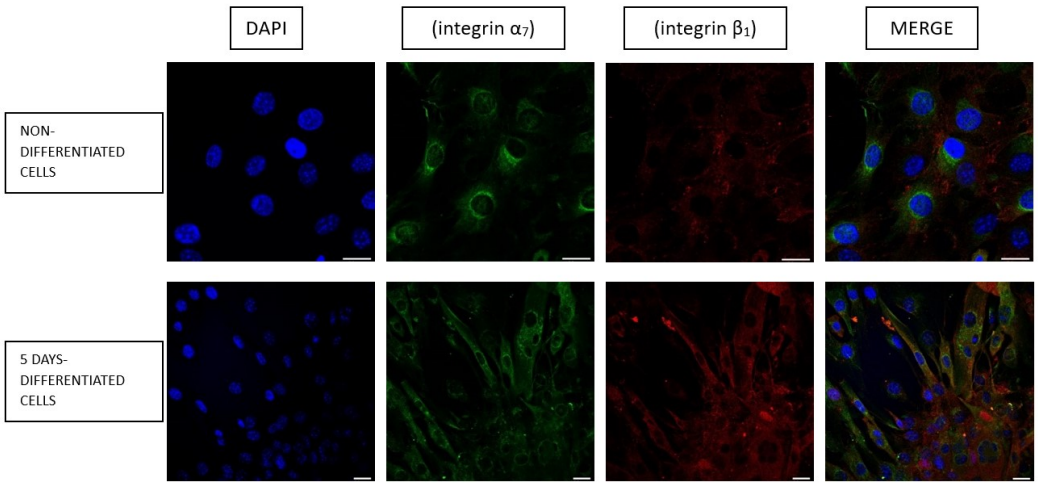

Figure 3.1: Immunostaining of integrins α_7 and β_1 in non differentiated C2C12 and 5-days differentiated C2C12. The scale bar in the image correspond to 20 μm.

The blue fluorescence signals are given by the DAPI and indicate the nucleus of cells. The green signals show the α_7 integrin subunit, whereas the red ones point to β_1. It can be noticed the different location of the integrins comparing the non-differentiated cells and the differentiated ones. In the first case, the signal is lower and more concentrated around the nucleus, whereas in the second case, the images show a higher expression of the integrins, distributed now throughout the entire cellular membrane. Another important element displayed is that the differentiated cells, after 5 days, present themselves as multi-nucleus myotubes with the typical elongated shape.

Moreover, we analysed the expression of Desmin, often used as a differentiation marker [32] (**figure 3.2**).

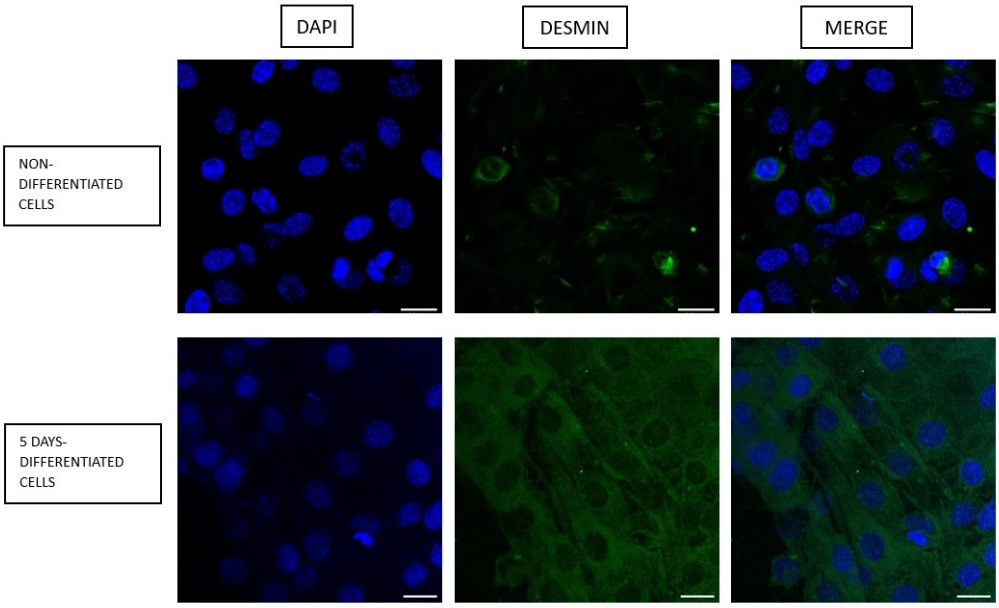

Figure 3.2: Immunostaining of Desmin in non differentiated C2C12 and 5-days differentiated C2C12. The scale bar in the image correspond to 20 μm.

The blue signals are given again by the DAPI and the green ones show the Desmin. The images underline the differentiation process occurred and show the myotubes. It was fundamental for our following experiment to verify the differentiation process of C2C12 after 5 days and to confirm the presence of the integrin $\alpha_7\beta_1$, since it was the chosen target of our NPs.

3.2 Synthesis and characterization of OM-pBAEs NPs

Another fundamental step for our project was the synthesis and the characterization of the NPs. Their size, polydispersity index (PDI) and zeta potential (Z-potential) were analysed by the DLS. The size was also evaluated by the NTA. The data obtained are represented in the graphics below (**Figure 3.3**).

The size of the NPs shown by DLS analysis is between 150 nm and 200 nm, whereas the values from NTA are slightly lower. This difference could be given by the fact that the NTA has a higher resolution, since it tracks individually the NPs and the results of DLS are more affected by the bigger NPs. Regardless, the size of the NPs was acceptable to perform uptake experiments in vitro. PDI is around 0.2, indicating that the samples were monodisperse. Regarding the Z-potential, this goes between 15 mV and 20 mV, which is what we were expecting given the nature of the OM-pBAEs. It's important to notice that the Z-potential did not change significantly adding the targeting peptides. The Z-potential of the zwitterionic NPs should be less positive, but this measurement can have a certain variability due to the fact that the Z-potential itself is quite variable and strongly depends by temperature and pH. Additionally, the position of the polymers in the NPs can change, altering the charge of the surface. Cationic peptides, as K and H, increase the positive surface charge of the NPs and a consequence is low selectivity during transfection: they will have interaction with any cell membrane since it is negatively charged due to the anionic phospholipid bilayer [26][27]. The zwitterionic NPs should have a lower positive charge and therefore a reduced tendency to transfect so easily. For this reason we would expect lower uptakes from these NPs comparing to the non zwitterionic ones. This agrees with our intent that is to have NPs that target specifically muscle cells thanks to the targeting peptides.

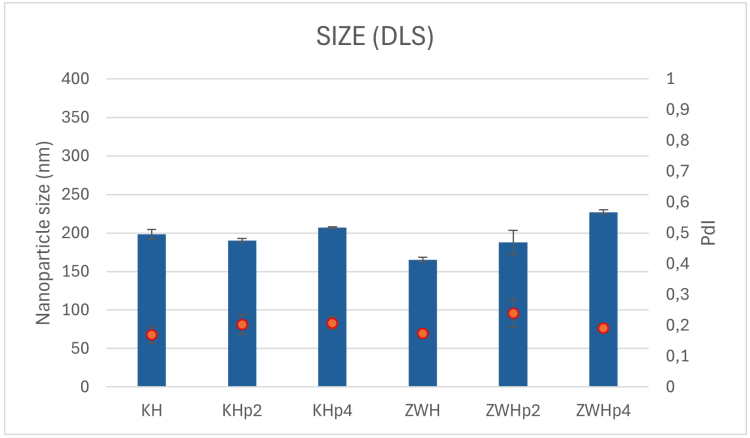

(A)

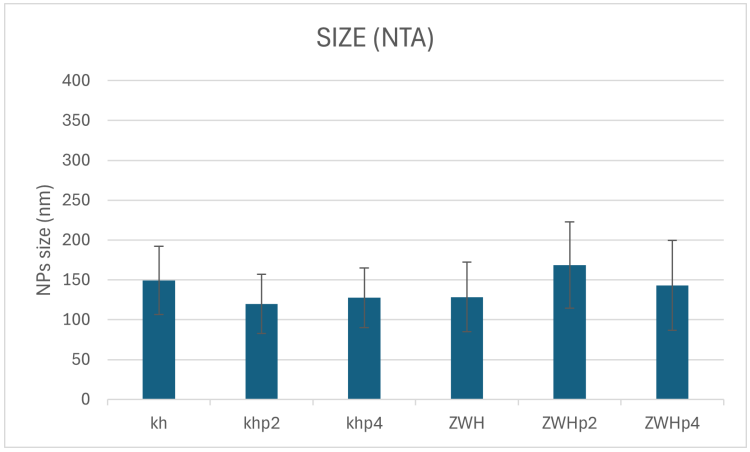

(B)

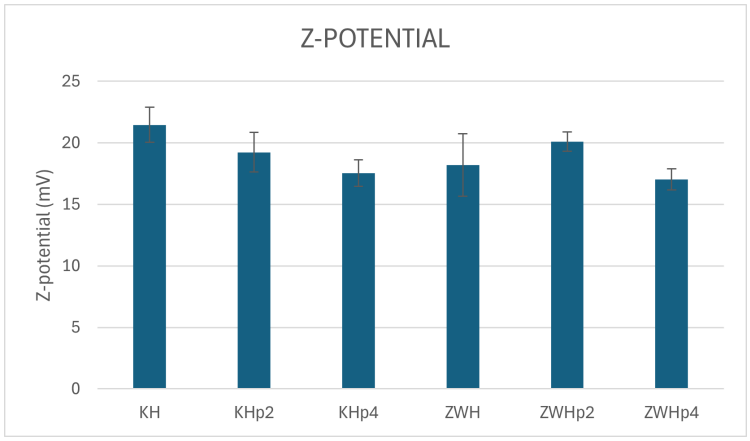

(C)

Figure 3.3: Characterization of the size of NPs by DLS (A) and by NTA (B). Characterization of Z-potential of NPs by DLS (C). In (A) it is also shown the PDI (red dots).

3.3 Uptakes with OM-pBAEs NPs

The core of this project involves the uptake experiments, both with non-differentiated and differentiated cells. We wanted to understand if the NPs were being internalized in the cells efficiently, which was the best timing and which compositions of NPs were more effective. We tested all the compositions of NPs described in **Table 2.3** and different incubation timings: 2, 4, 6 and 8 hours. Regarding the differentiated cells, we also waited for a longer time, leaving the NPs to incubate overnight. All the experiments were repeated three times and each sample was in triplicate. Using OM-pBAE NPs, there should be a quite high uptake because of their positive charge. The ideal result would have been an higher uptake with the NPs with the targeting peptides because their internalization would be also and especially given by the specific interaction with the integrin $\alpha_7\beta_1$. This should have been noticed particularly with the differentiated cells, that have indeed a greater expression of the target. Moreover, we could have expected a lower uptake with the zwitterionic NPs, since they should be less positive than the classic OM-pBAE NPs. However, the results obtained by flow cytometry and displayed in **Figure 3.4** and **Figure 3.7**, partly differ from our suppositions.

3.3.1 Uptakes with non-differentiated cells

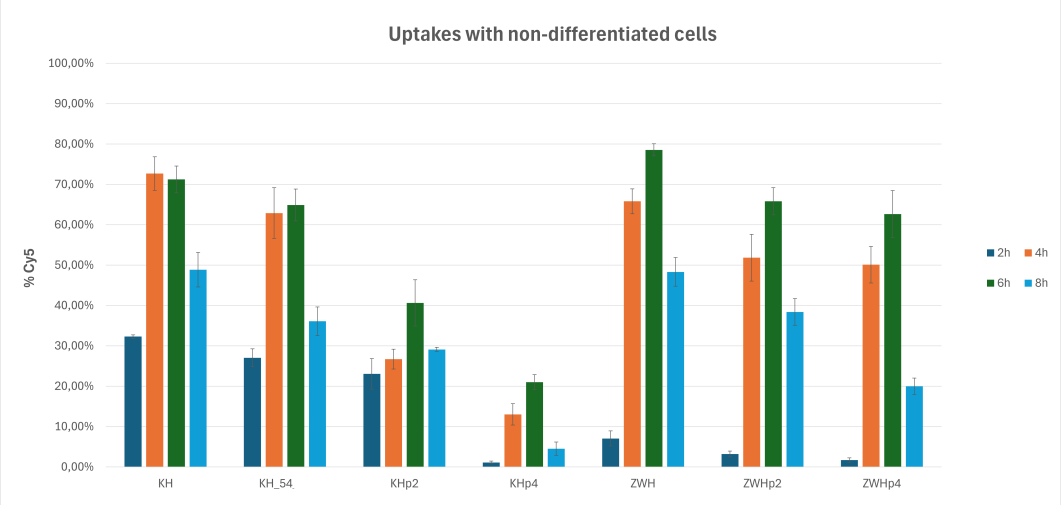

Figure 3.4: Uptakes efficiency (% Cy5) after of 2, 4, 6 and 8 hours of incubation with NPs containing PGFP labelled with Cy5. The experiment was done with non-differentiated C2C12 and the NPs used are KH, KH_{54}, ZWH, ZWHp2, ZWHp4.

Regarding non-differentiated cells, we can focus firstly on the uptakes with the non zwitterionic NPs. We can observe that, after 2 hours of incubation, there is already a significant entrance, between 20% and 30%, in the cells. With an incubation time of 4 hours, the uptake of PGFP was substantially higher, reaching 60%-70%, with the exception of KHp2, where it doesn't increase notably. Actually, observing the results of KHp2, but also of KHp4, their uptakes are lower in any incubation

time compared to KH and KH_{54} and they don't increase a lot incrementing the timing. After 6 hours, there is a general growth of the uptakes, around 60%-70% for KH and KH_{54}. Lastly, after 8 hours of incubation, we noticed a decrease of the uptake of PGFP, which was not expected. Looking now the zwitterionic NPs, after 2 hours of incubation, the uptakes are quite low, around 5%. This difference with the non zwitterionic NPs does not conflict with the fact that, as mentioned above, the zwitterionic NPs are entering in the cells more slowly, given their lower positive charge. After 4 hours, their uptakes are more similar to the ones of the other group of NPs: it is possible to observe a significant increase of the uptakes that are between 50% and 60%. After 6 hours, there is still an increase of the uptakes that go above 60%. ZWH even arrives almost at 80%. After 8 hours, even with the zwitterionic NPs, is possible to notice a decrease of the uptakes. A possible explanation could be the degradation of the polymer of the NPs or that they have started to exit the cells, but the real motivation require a deeper investigation. We observed this trend also with the qualitative analysis of the localization of the NPs during different uptakes, deepened in the following section. KH and KH_{54} represent a positive control because we know that KH, that is composed by 60% of K and 40% of H, is internalized efficiently [27]. We chose to synthesize also KH_{54}, which has a very similar composition (54% of K and 46% of H), because it has the same amount of K present in KHp2 and KHp4. We wanted to verify if this minor difference had some effect on the uptake, but the results of KH and KH_{54} are quite similar, in the case of both non-differentiated and differentiated cells. It may be noticed that the uptake with KH_{54} is slightly lower regarding the non-differentiated cells, but not in a significant way. A low amount of KHp2 and KHp4 seem to enter the cells, as already noted. The difference between the behaviours of these NPs and KH and KH_{54} suggest that the NPs are different and thus that led us to think that the targeting peptides are encapsulated in the NPs. If they weren't, all four would have given similar results. At the same time, they do not present higher uptakes, so it doesn't seem that the targeting peptides are really working, but we expected that this could happen with the non-differentiated cells. We can observe this also between the zwitterionic NPs with the targeting peptides and without, but the difference in the uptakes is minor.

3.3.2 Localization of NPs during the uptakes

Regarding the DNA uptakes with the non-differentiated cells, besides the quantitative analysis with the flow cytometry, we decided to examine it qualitatively with the confocal microscope. We chose to study all the NPs and three incubation time: 2 hours, 4 hours and 8 hours. We decided to exclude the 6 hours incubation since the results were similar to the uptakes of 4 hours. The results obtained were almost completely consistent with the ones analysed in the previous section, as displayed in the following images (**Figure 3.5**). The red signals, given by the PGFP labelled with

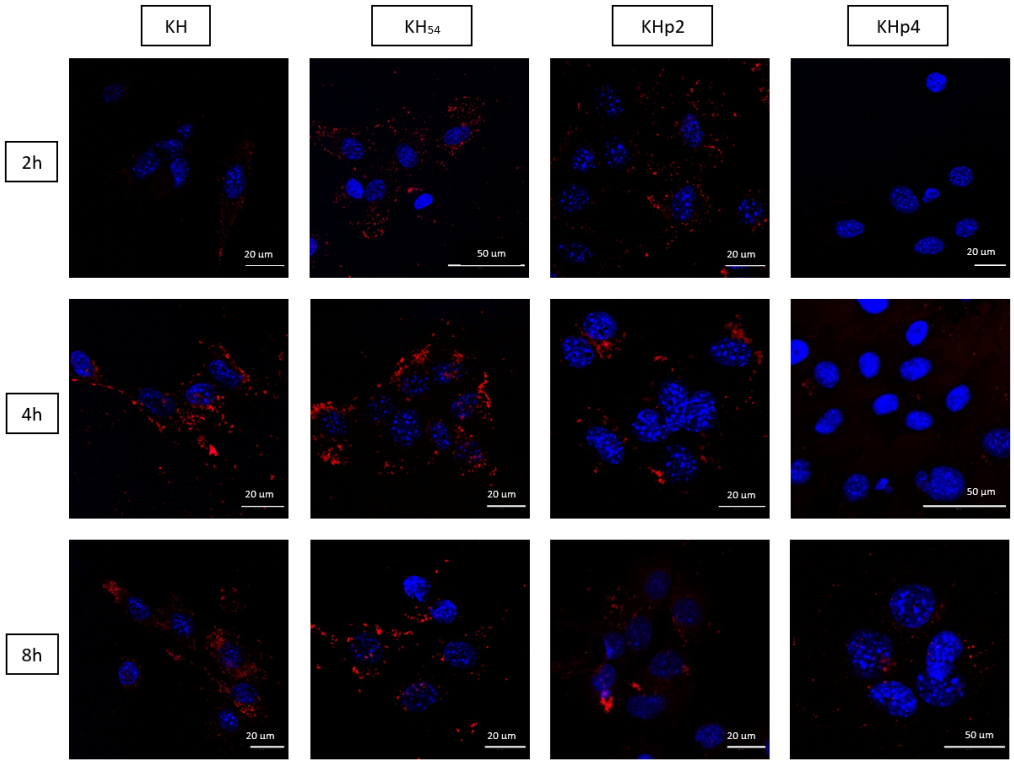

Figure 3.5: Images obtained with the confocal microscope. The blue signal is given by the DAPI and indicates the nucleus of the cells, while the red one is given by the PGFP labelled with Cy5 encapsulated in the NPs. Here there are the images of the uptakes after 2, 4 and 8 hours of incubation with the KH, KH_{54}, KHp2 and KHp4.

Cy5, are almost absent in the uptake of 2 hours, while in the one of 4 hours it can be noticed easily. As shown in the previous graphic, KHp2 and KHp4 are entering with more difficulty than KH and KH_{54}. Specifically, the uptake with KHp4 seems almost null, since it is possible to see very few red dots. As mentioned in the prior section, it is possible to notice also here that the entrance of the NPs after 8 hours seems lower than after 4 hours. It is also to be considered that this experiment has been effectuated only one time with a duplicate for each sample, since it is quite difficult to maintain the cells attached to the cover glass. But still, the results are consistent with the quantitative ones. It is possible to see that the PGFP, and thus the NPs, entered the cells and are distributed in the cytoplasm. In some cases it is possible to notice that some PGFP is in the nucleus.

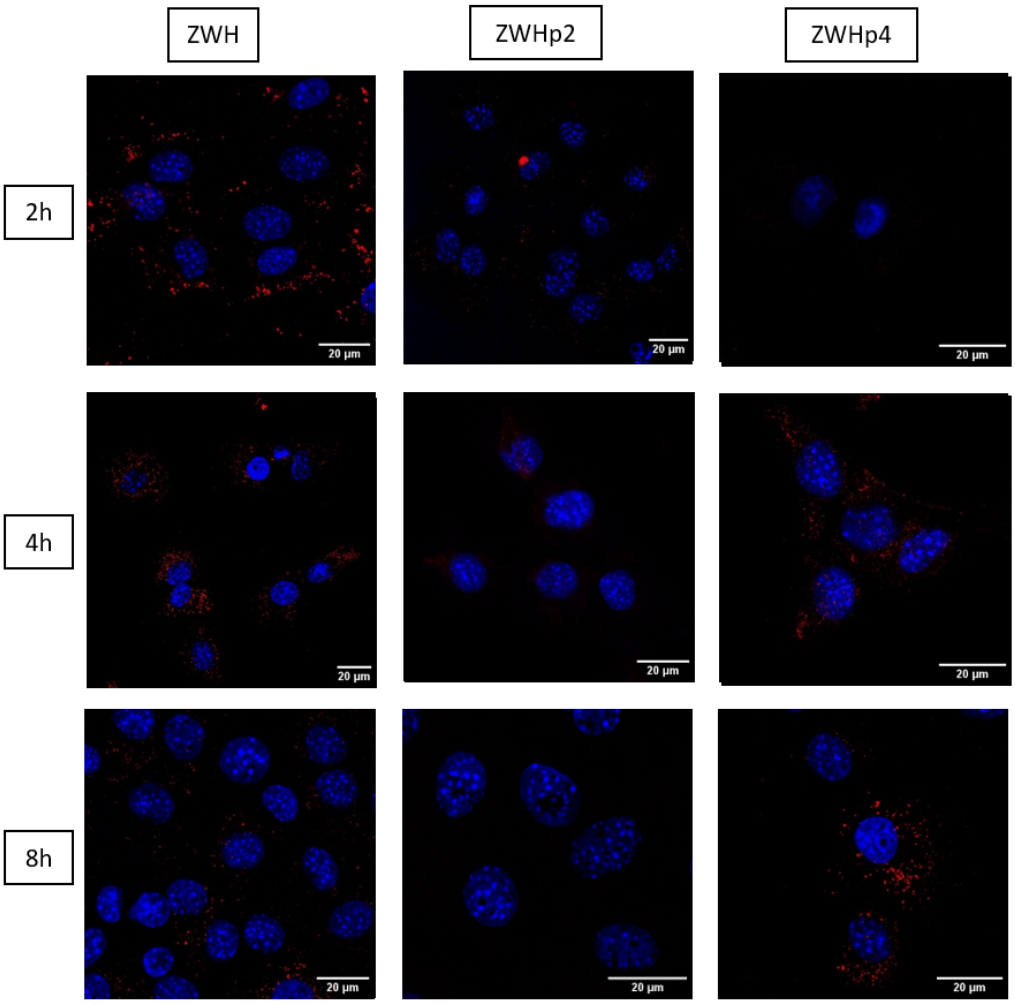

Figure 3.6: Images obtained with the confocal microscope. The blue signal is given by the DAPI and points to the cell nucleus. The red signal indicates the PGPF labelled with Cy5 encapsulated in the NPs. Here there are the uptakes with 2,4 and 8 hours of incubation with the zwitterionic NPs: ZWH, ZWHp2 and ZWHp4.

Regarding the zwitterionic NPs, shown in the **Figure 3.6**, the results obtained by the confocal analysis are quite different by the ones taken with the flow cytometer. It is important to point out that here the images have being modified comparing to the previous ones: the brightness of the the red signals has being increased. The settings are different only between the zwitterionic NPs and the non zwitterionic ones. Among the two groups, the settings are the same. This decision was made because the red signals in this case were really low and they would have not being seen at all using the same brightness in most cases. Taking the pictures with the microscope, we noticed that, even if really weak, some red signals were present and we decided to underline this and represent them in this way. Since the settings are different, the images cannot be compared, but the purpose of this experiment was to compare these results with the prior ones and to actually visualize where the PGFP would localize in the cells. The labelled PGPF entered in the cells is very few and this follows the quantitative datas as for the uptake of 2 hours. After 4 hours, looking

at the graphic (**Figure 3.4**), there should be more red signal, as the uptakes had similar values to KH and were around 50%-60%. After 8 hours of incubation, the uptakes seem similar to the ones of 4 hours, in the case of ZWH it appears even with a little less signal.
There is some discrepancy between the results obtained with the confocal microscope and the ones found with the cytometer. The confocal analysis was important because it allowed us to have actual images of what was happening, but it was a qualitative analysis. The pictures we chose to show are the ones that represented better the whole samples, but of course there were parts were the signals were slightly higher or lower. Moreover, while the cytometry experiments were repeated multiple times with triplicate, the confocal ones were only effectuated one time with duplicates. Thus, the cytometry analysis, which are quantitative, are more reliable.

3.3.3 Uptakes with differentiated cells

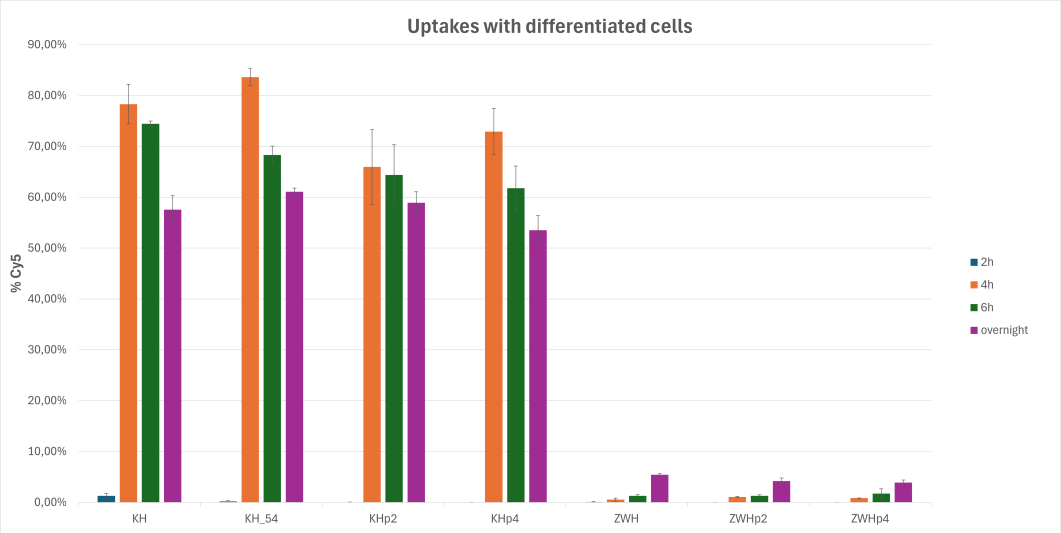

Figure 3.7: Uptakes efficiency (% Cy5) after an incubation of 2, 4, 6 hours or overnight with NPs containing PGFP labelled with Cy5. Here it's shown the uptake with differentiated cells and the NPs used are KH, KH_{54}, ZWH, ZWHp2, ZWHp4.

Regarding the differentiated cells, analysing the results given by the flow cytometer, we decided to investigate also a longer incubation time leaving the NPs with cells overnight and replacing the one of 8 hours. After 2 hours of incubation, the uptake is almost null. Considering the non zwitterionic NPs, after 4 hours a significant increase can be noticed and it is maintained also after 6 hours. Their values are quite similar to the corresponding uptakes with the non-differentiated cells. Here, KHp2 and KHp4 seem to enter nearly as KH and KH_{54}, but their uptakes are still not higher. With the overnight uptakes, the values decrease, but they remain over 50%. Regarding the zwitterionic NPs, they all present very little uptakes, almost null. It is possible to see some uptake leaving the NPs to incubate with the cells overnight, even if it is still under 10%, so very few NPs are internalized.
Analysing the general results, we can observe that the differentiated cells seem more difficult to enter comparing to the non-differentiated ones, probably because of changes of the cell membrane and the cytoskeleton that occur during the differentiation process. Moreover, we can observe again that the targeting peptides are not ensuring a higher uptake even with the differentiated C2C12. Since the targeting peptides are shown to be efficient [29], our results led us to think that something is not working as we wanted. The peptides could be not encapsulated in a correct way in the NPs or they could be not well exposed. As mentioned above, the peptides seem to be encapsulated in the NPs, since the uptakes of the NPs with them and the ones without differ, but it has to be verified.

3.4 Colocalization analysis of genetic material and polymer in the NPs

We relied again on confocal microscope analysis to investigate one of the questions raised by the uptakes experiments. To understand if the targeting peptides were well encapsulated in the NPs, we decided to verify their position related to that of the PGFP. If they are both present and if they colocalize it means that P2 and P4 are encapsulated. As explained in the **section 2.11**, for this experiment we labelled the polymers with the targeting peptides (C6-P2 and C6-P4) and C6-H with Cy3 besides the PGPF with Cy5. We investigated KHp2, KHp4, ZWHp2 and ZWHp4. For each type of NP, we analysed one NP with the polymers with targeting peptides labelled and another one with C6-H3 labelled, that functioned as control. PGFP was always labelled (**Figure 3.10**).

Since in each sample there were two elements with a fluorophore, we needed to know the quantity of both Cy3 and Cy5 in the NPs to ensure that in each one there was a comparable amount of the two fluorophores. Once the labelled polymers and PGFP were ready, we needed to determine the concentration of Cy3 or Cy5. To do so, we had to plot the calibration curve. Starting with Cy5, we prepared six standards with serial dilutions (1:10), starting from 99 μL of PBS and 1 μL of Cy5 (10 mg/mL). We measured their fluorescence intensity with Infinite® 200 PRO (Tecan) plate reader and we plotted the calibration curve (**Figure 3.8**).

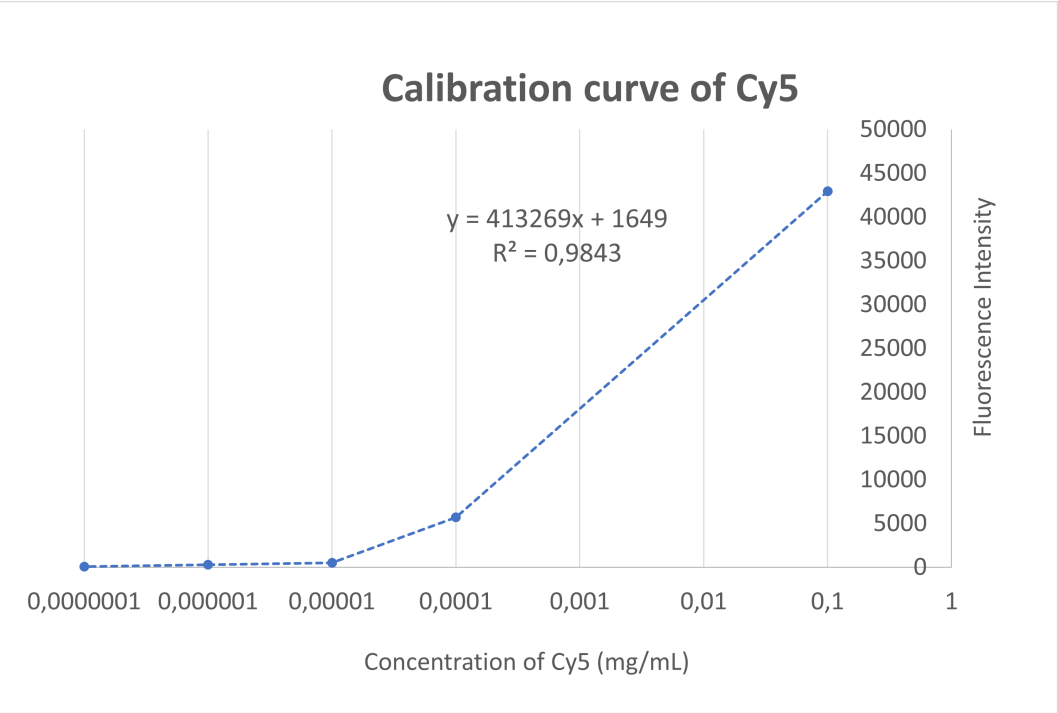

Figure 3.8: Calibration curve of Cy5.

We then prepared three dilutions (1:10) of the labelled PGFP, starting from 99 μL of PBS and 1 μL of the sample and we measured their fluorescence with the plate reader. Knowing the concentration of PGFP of the three dilutions and their corresponding fluorescence intensity, thanks to the calibration curve, we could calculate the concentration of Cy5 in our sample with the following calculation (**Equation 3.1**):

$$C_{Cy5,dil} = (y - q)/mC_{Cy5} = C_{Cy5,dil} * dil \tag{3.1}$$

Equation 3.1: Equation to calculate the concentration of Cy5.

where $C_{Cy5,dil}$ is the concentration of Cy5 in the dilution (mg/mL), y is the fluorescence intensity of one of the three dilution of the sample, q and m are coefficients given by the calibration curve (q = 1649; m = 413269), dil is the dilution and C_{Cy5} is the concentration of the non diluted sample. After, we used the same machine with NanoQuant Plate™ to know the concentration of PGFP. We then diluted it with MilliQ water to have a 1 mg/mL concentration. We utilized the same procedure to obtain the concentration of Cy3 in the three different labelled polymers, plotting the following calibration curve (**Figure 3.9**):

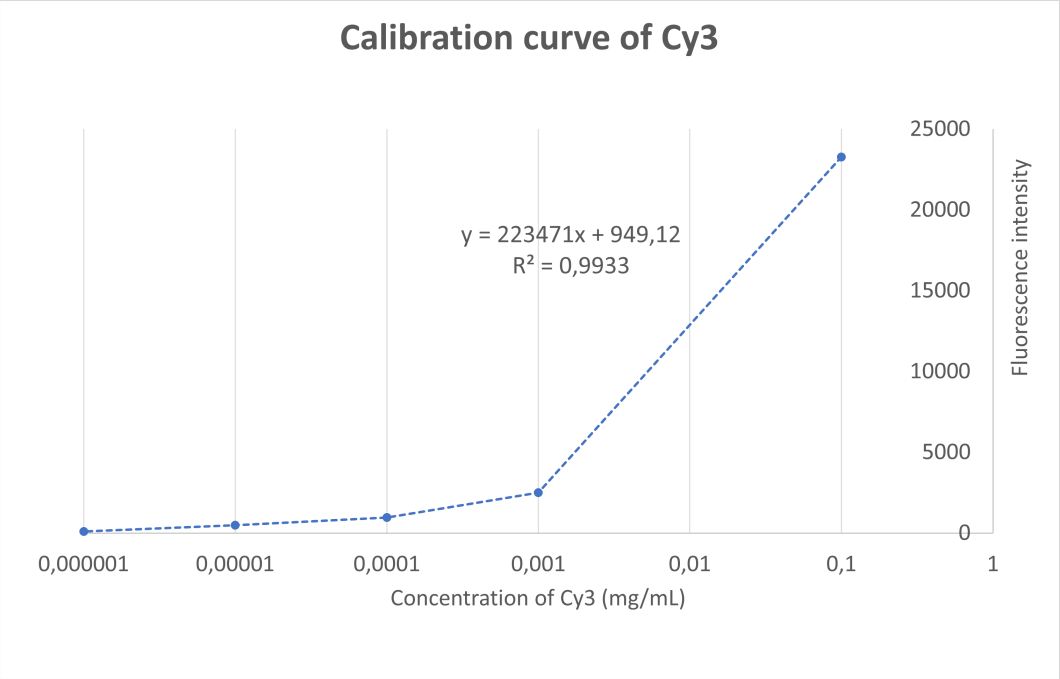

Figure 3.9: Calibration curve of Cy3.

The obtained concentrations are the following (**Table 3.1**):

Labelled polymers	**Concentration of Cy3 (mg/mL)**
C6-H	13,5
C6-P2	7,98
C6-P4	19,6

Table 3.1: Concentration of Cy3 (mg/mL) in the labelled polymers C6-H, C6-P2 and C6-P4.

These concentrations are very high compared to the that of Cy3 in the PGFP sample, which is 0,286 mg/mL. Since our experiment is to understand if the targeting peptides are encapsulated in the NPs in a qualitative way, it is not strictly necessary that the concentrations of the different fluorophore are exactly the same, but they need to be quite comparable. It is also better if the grams of Cy5 and Cy3 in a NP are the same. Another aspect to consider is that the different polymers and also the PGFP are put in the NPs with different percentages. Therefore, for example, 1% of the genetic material will be different compared to 1% of C6-H present in the NPs. For all these reasons, we needed to understand the correct dilutions of the labelled polymers and genetic materials to use. Firstly, we decided to increase the usual amount of labelled PGFP, from a dilution of 1:100 to a one of 1:10 (10% of labelled PGFP and 90% of non labelled PGFP). Then, we calculated the grams of Cy5 present in a NP of 45 μL and the concentration of diluted Cy5. Knowing this, wanting the same amount of Cy3, we determined the percentage of the labelled polymers that had to be in the NPs and the concentration of the diluted Cy3 with the following calculations (**Table 3.2**):

NP of 45 μL				
PGFP	C_{Cy5} =		0,286	mg/mL
	Volume of PGFP in a NP of 45 μL (V_{PGFP})		3,75	μL
	Concentration of Cy5 with 10% of labelled PGFP	$C_{Cy5}/10$ =	0,0286	mg/mL
	μg of Cy5 (M_{Cy5})	0,0286*V_{PGFP}	0,107	μg
C6-H	C_{Cy3_H} =		13,5	mg/mL
	Volume of C6-H in a NP of 45 μL (V_H)		0,34	μL
	Concentration of Cy3 once diluted ($C_{Cy3_H dil}$)	V_H/M_{Cy5} =	0,315	mg/mL
	%C6-H labelled	($C_{Cy3_H dil}/C_{Cy3_H}$) * 100 =	2,33	%
C6-P2	$C_{Cy3_P 2}$		7,98	mg/mL
	Volume of C6-P2 in a NP of 45 μL (V_{P2})		0,094	μL
	Concentration of Cy3 once diluted ($C_{Cy3_{P2} dil}$)	V_{P2}/M_{Cy5} =	1,14	mg/mL
	%C6-P2 labelled	($C_{Cy3_{P2} dil}/C_{Cy3_{P2}}$) * 100 =	14,3	%
C6-P4	$C_{Cy3_P 4}$		19,6	mg/mL
	Volume of C6-P4 in a NP of 45 μL (V_{P4})		0,094	μL
	Concentration of Cy3 once diluted ($C_{Cy3_{P4} dil}$)	V_{P4}/M_{Cy5} =	1,14	mg/mL
	% P4 labelled	($C_{Cy3_{P4} dil}/C_{Cy3_{P4}}$) * 100 =	5,81	%

Table 3.2: Calculation to understand the percentage of labelled polymers to use in the synthesis of the NPs to have the same amount of the fluorophores Cy3 and Cy5.

The different concentrations are still slightly different, but for our purposes, these values were acceptable and we actually had reasonable results, as shown in **Figure 3.10** and **Figure 3.11**. For this experiment, we decided to use non-differentiated C2C12, since they stay more easily attached to the cover glasses necessary for the confocal analysis and we examined an uptake of 4 hours. In general, analysing these images, we can say that the targeting peptides entered the cells and in some cases, it is possible to see the colocalization with PGFP. In the case of the zwitterionc NPs, the PGFP and the polymer signals result weaker, but this goes accordingly with what we analysed during the uptake experiments. This

experiment helped us to see if the targeting peptides were actually being encapsulated in the NPs and the answer is positive. In the next images (**Figure 3.10**) is shown a schematic representation of the NPs studied in this experiment, followed by the actual confocal microscope images (**Figure 3.11** and **Figure 3.12**).

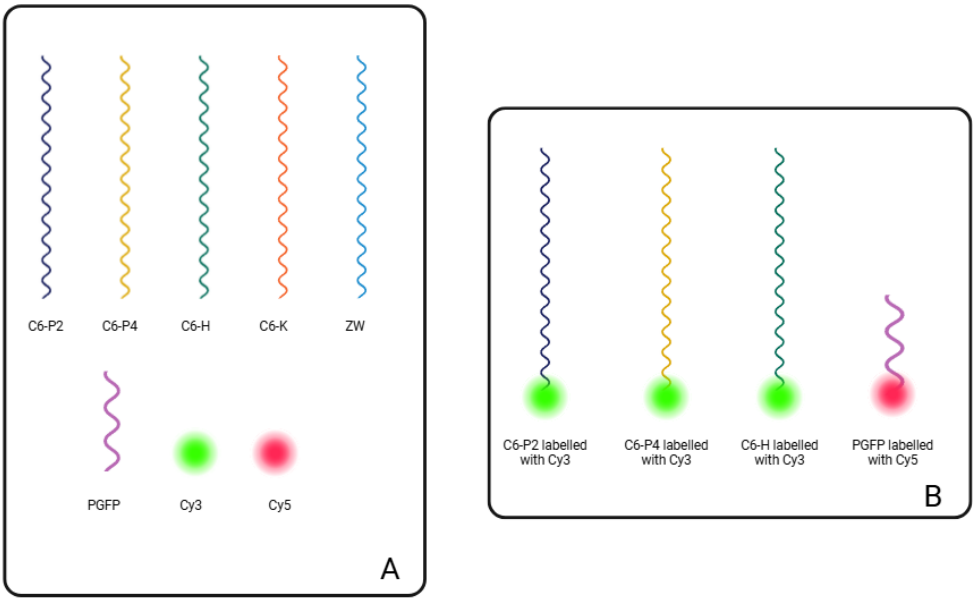

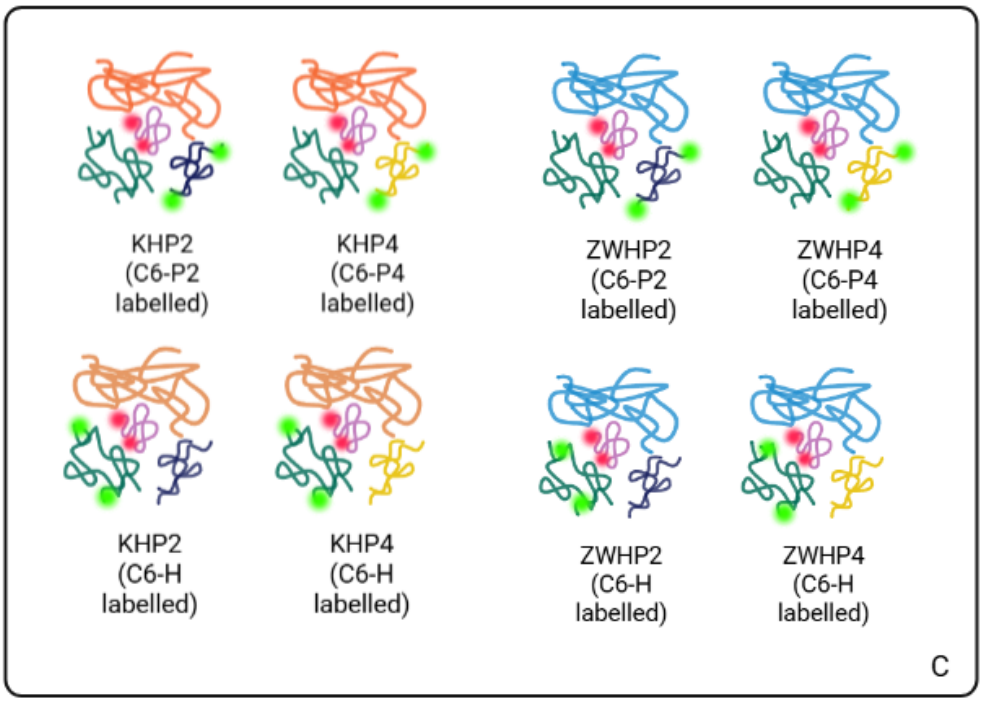

Figure 3.10: Schematic representation of labelled polymers and of the composition of the NPs synthesized for the colocalization experiment. A) Representation of the polymers, the genetic material and the fluorescent dyes Cy3 and Cy5 used: C6-P2 (dark blue), C6-P4 (yellow), C6-H (green), C6-K (orange), ZW (light-blue), PGFP (pink), Cy3 (green sphere) and Cy5 (red sphere). B) C6-P2, C6-P4 and C6-H were labelled with Cy3, while PGFP was labelled with Cy5. C) NPs analysed in this experiment: KHP2, KHP4, ZWHP2 and ZWHP4. PGFP was always labelled. For each type of NP, we analysed them once with C6-P2 (or C6-P4) labelled and then with C6-H labelled.

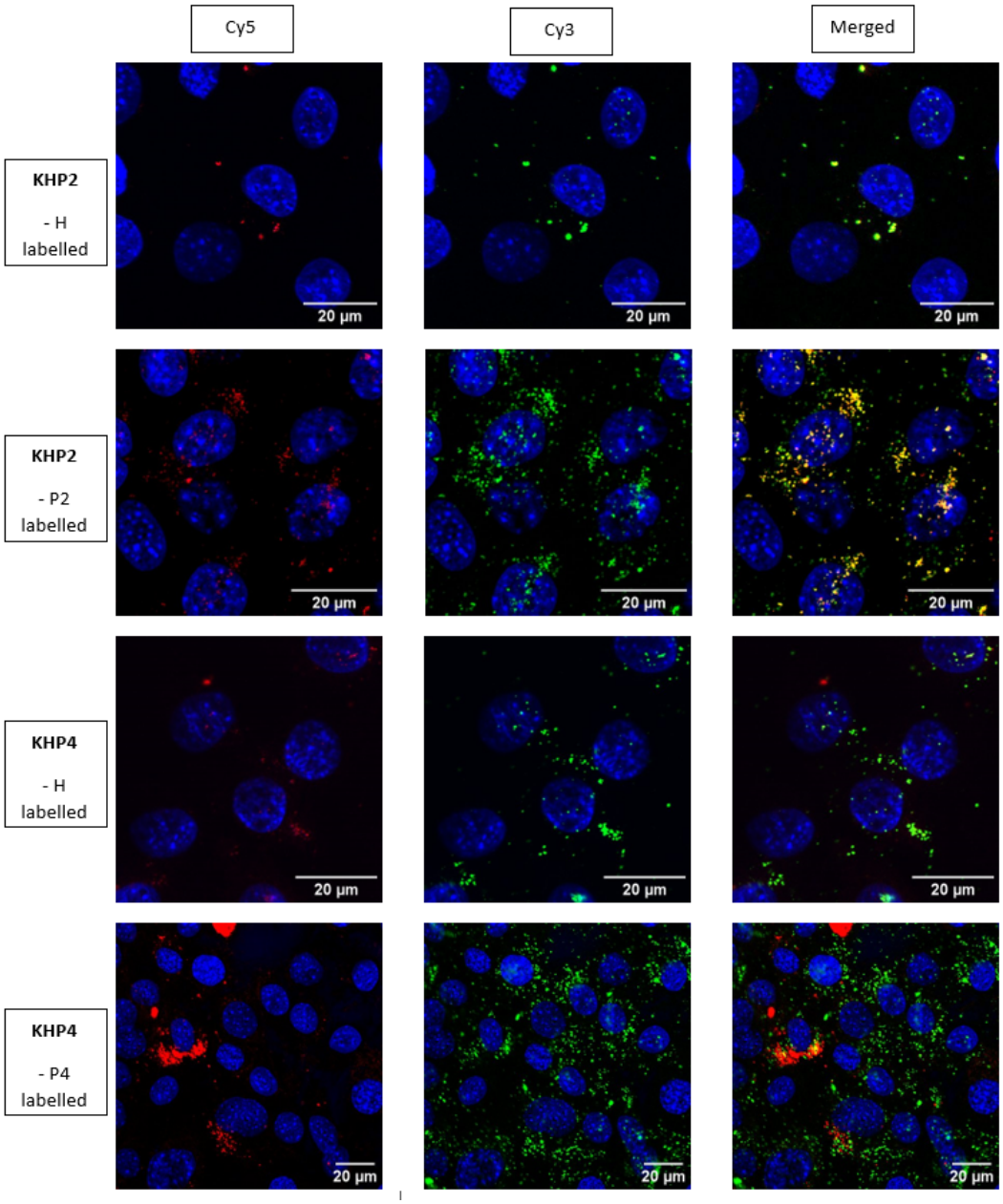

Figure 3.11: Confocal microscope images of a 4 hours uptake with with KHp2 and KHp4 non-differentiated C2C12. The blue fluorescence is given by the DAPI and indicates the nucleus of the cells, while the red signals indicate PGFP labelled with Cy5 and the green one indicate the Cy3-labelled polymer, C6-H or C6-P2. In the third column there are both red and green signals that, if they colocalize, are represented in yellow.

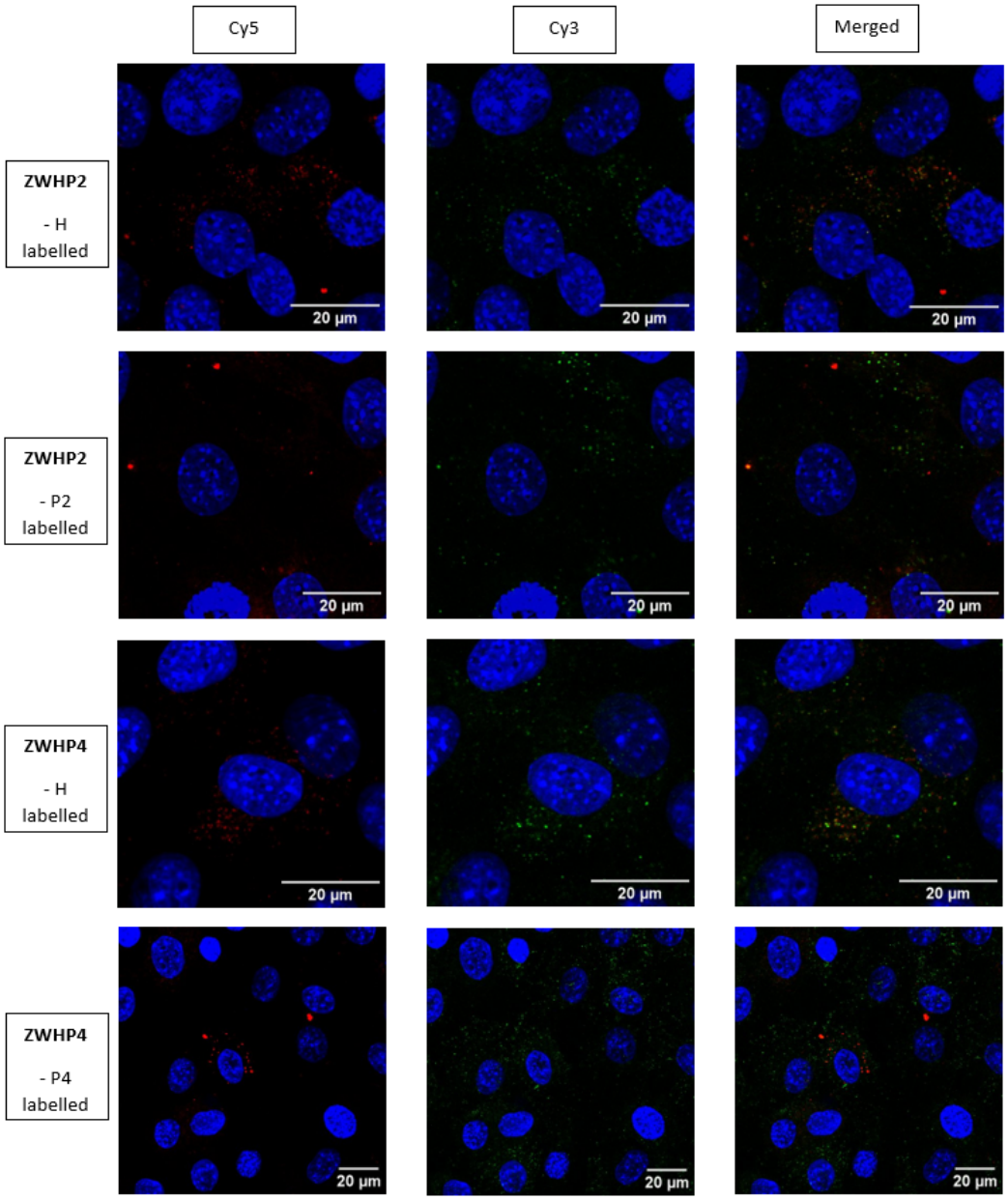

Figure 3.12: Confocal microscope images of a 4 hours uptake with ZWHp2 and ZWHp4, with non-differentiated C2C12. The blue fluorescence is given by the DAPI and indicates the nucleus of the cells, while the red signals indicate PGFP labelled with Cy5 and the green one indicate the Cy3-labelled polymer, C6-H or C6-P2. In the third column there are both red and green signals that, if they colocalize, are represented in yellow.

3.5 Competition experiments

Once verified that the targeting peptides were well encapsulated in the NPs, the second aspect to investigate was if the targeting peptides were binding with the integrin $\alpha_7\beta_1$ or not. As already mentioned, if they were not targeting the integrin, it was probably because they were not well exposed. Hence, we performed a competition experiment between the NPs with the targeting peptides and the free peptide. The idea was to have a pre-incubation of the free peptide with the cells and only later to add the NPs. In this way, if the NPs were specifically targeting the cells, the uptakes should be lower since the integrins have already bound with the free peptides. We chose to use P2. As explained in **section 2.9**, we calculated the amount of P2 to add to the cells, which corresponded to the amount of targeting peptide present in the NPs. We decided to have three parallel uptakes: one without adding the free peptide (indicated as P*0 in the graphics), one adding the calculated amount (referred to as P*1) and the last adding twice the amount (listed as P*2). The first one is our control. Initially, looking at the literature [33], we tried a 30 minutes pre-incubation time, but then we decided to wait for more time, so we tried also to incubate the free peptide for 60 minutes. As incubation time for the NPs, we decided for 6 hours for the non-differentiated cells, while for the differentiated ones we decided to let the NPs with the the cells overnight. In these experiments, we chose to stop using both KH and KH_{54}, preferring only the second one, since the results from the previous uptakes were similar. Initially, we diluted the peptide in DMSO, but observing the

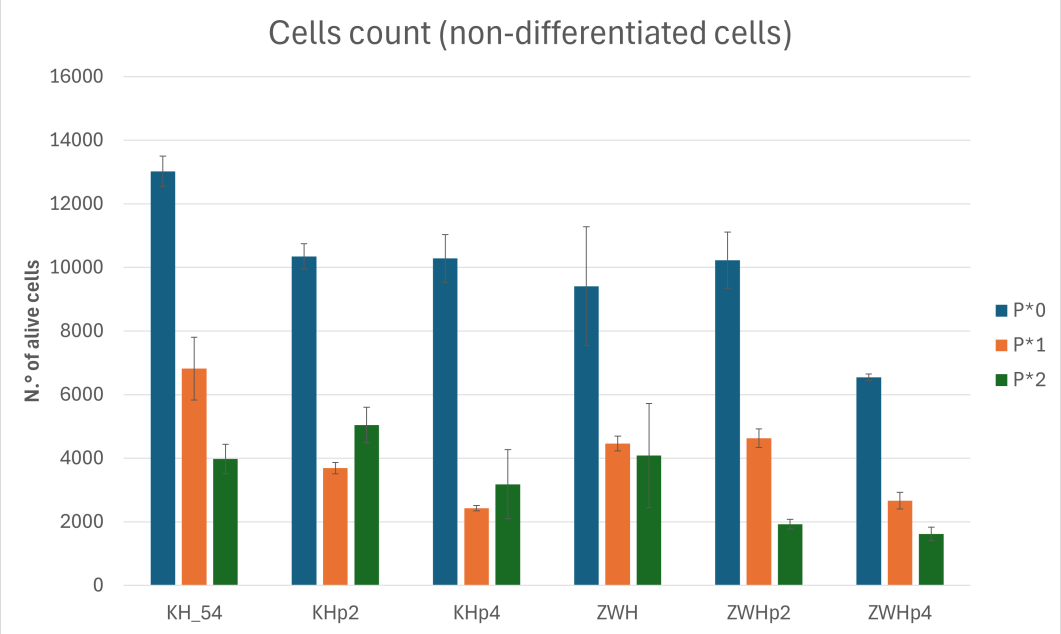

Figure 3.13: Cell count of the uptake of 6 hours with non-differentiated cells, done for the competition experiment. The peptide here was pre-incubated 30 minutes and it was diluted in DMSO.

cell count, we noticed that maybe it was toxic for the cells. In fact, with the first competition experiment, done with non-differentiated cells and with a pre-incubation

time of 30 minutes, it is possible to notice how the number of alive cells decreases significantly from the uptake done without adding the free peptide and the other two uptakes (**Figure 3.13**). The number of cells is halved, or even more reduced in some cases. For example, analysing the uptakes with KH_{54}, the flow cytometer counted between 12000 and 14000 alive cells for P*0, while with P*2 the count is around 4000. Or again, with KHp2, KHp4, ZWH and ZWHp2 the cells in P*0 are approximately 10000, whereas with P*1 and P*2 are nearly 4000. The uptakes done with ZWHp4 presents a lower number in general, but it is still possible to observe the diminishing of cells. For this reason, for the following experiments we diluted P2 in milliQ water. With this change, it is possible to observe that the number of cells remains quite stable comparing all the three different uptakes, both with non-differentiated and differentiated cells and even elongating the pre-incubation time (**Figure 3.14**, **3.15**, **3.16**). In the first and second graphics, the cells are around 10000 and the number stays mostly quite steady. In the last graphic, the competition experiment with differentiated C2C12 and the pre-incubation time of 60 minutes, the number of cells fluctuates more, but there is not a specific trend, as in **Figure 3.13**.

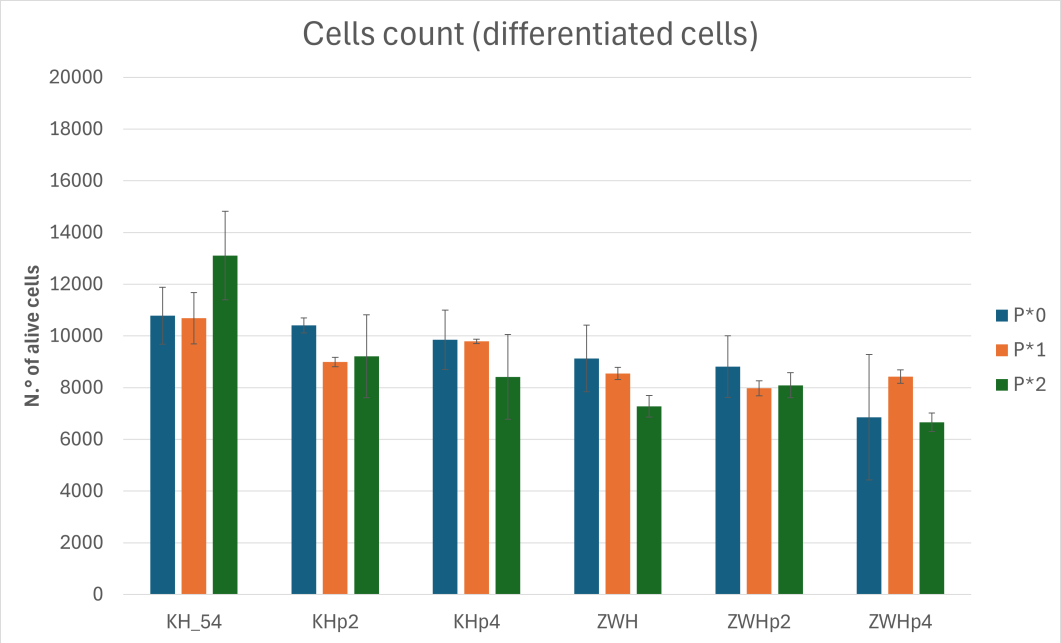

Figure 3.14: Cell count of the overnight uptake with differentiated cells, done for the competition experiment. The peptide here was pre-incubated 30 minutes and it was diluted in milliQ water.

Figure 3.15: Cell count of the uptake of 6 hours with non-differentiated cells, done for the competition experiment. The peptide here was pre-incubated 60 minutes and it was diluted in milliQ water.

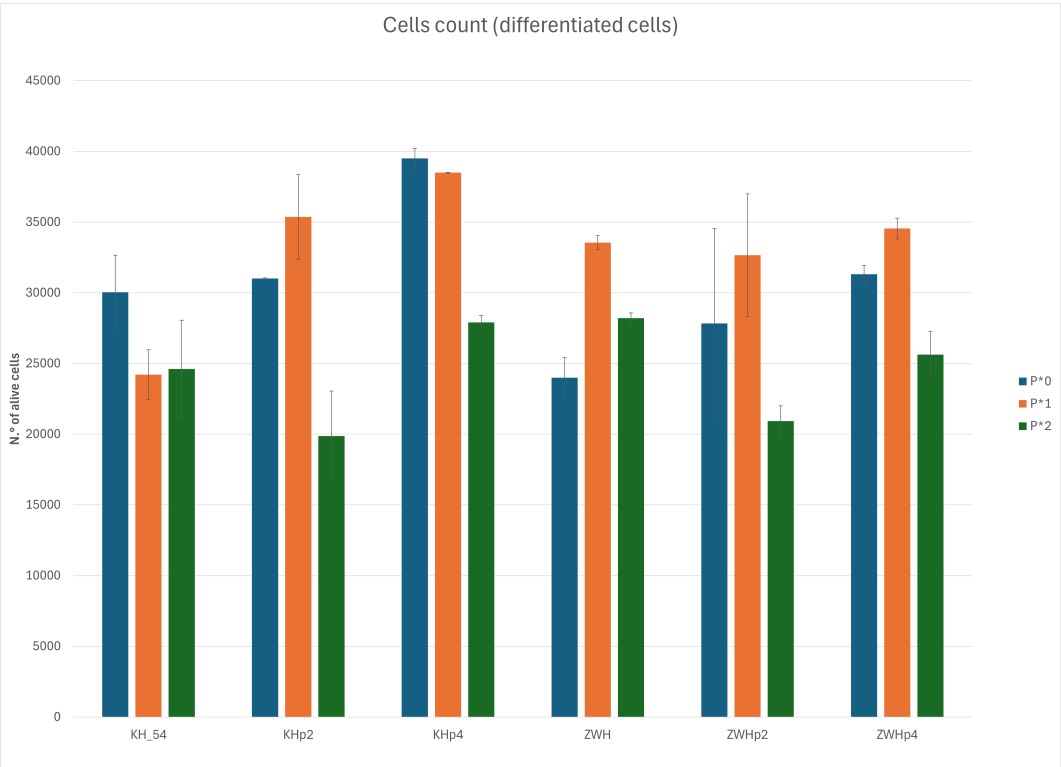

Figure 3.16: Cell count of the overnight uptake with differentiated cells, done for the competition experiment. The peptide here was pre-incubated 60 minutes and it was diluted in milliQ water.

Focusing now on the results of the uptakes, we expected to have similar results among the three different uptakes regarding the NPs without the targeting peptides, so KH_{54} and ZWH: the presence of the free peptide should not influence the entrance of these NPs, given only by the characteristics of the OM-pBAEs. On the contrary, the presence of free P2 should have lowered the uptakes of the NPs with the targeting peptides, that are meant to enter the cells also thanks to the specific targeting. Ideally, this difference should be more evident with the zwitterionic NPs, since they should count mostly on the specific targeting to enter the cells.
Regarding the first competition experiment done (**Figure 3.17**), the entrance of the NPs in the cells is quite low compared to the results obtained in the uptake experiments section. These datas are probably also influenced by the fact that the peptide was diluted in DMSO, leading a decrease in the number of cells. However, it is possible to observe that the uptake of KH_{54} remains basically unchanged, around 30% while with ZWH, the uptakes P*1 and P*2 are lower than P*0: P*0 is almost 30% and the other two are approximately 15%. With the uptakes with the targeting peptides it can be noted that P*0 is always higher than P*1 and P*2 (that are very similar), especially in the case of KHP2 and ZWHP4 P*0 is approximately the double of the other two uptakes. With KHP4 there isn't this difference and with ZWHP2 the uptakes are all very low. However, it is important to take into account that the number of cells is quite low and it doesn't allow a proper analysis.

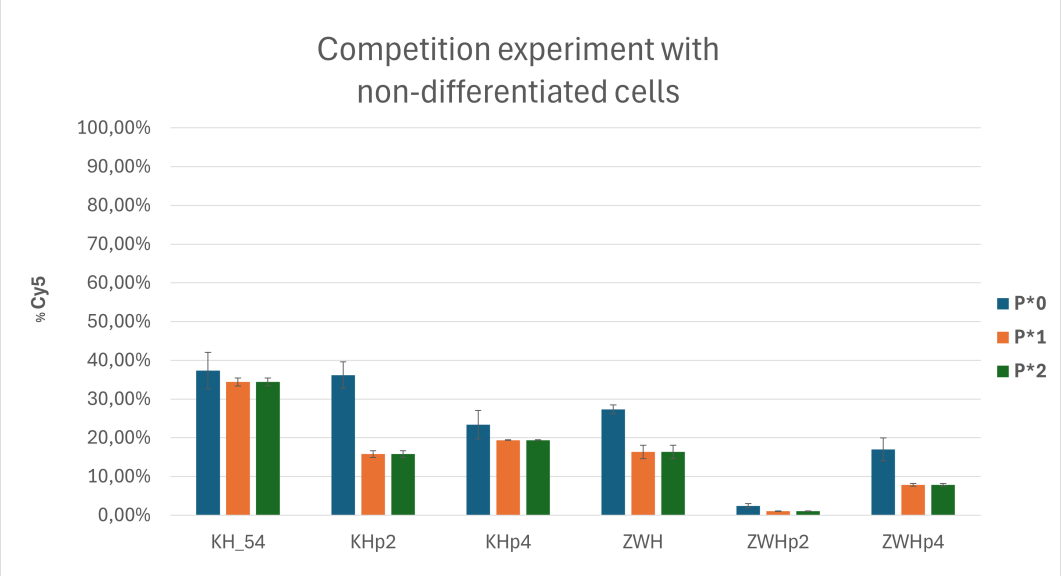

Figure 3.17: Competition experiment done with non-differentiated cells. The pre-incubation time was of 30 minutes and the following incubation time was 6 hours. In this case the peptide was diluted in DMSO.

The following experiment was done with differentiated C2C12 and the free peptide was diluted in milliQ water, as in all the other performed subsequently. The general results in this graphic (**Figure 3.18**) are quite far from what we expected both from our prediction and the previous results. The uptakes are very low with all the NPs: only P*2 with KH_{54} exceeds 30% and the zwitterionic NPs even present almost no uptake. In the **section 3.3.3**, leaving the cells overnight, the uptakes of the non-zwitterionic reach 50% and the zwitterionic ones are around at least 5%. Moreover, the entrance in the cells is higher in the uptakes where the free peptide is present: at most it should be the same. We decided to repeat the experiments with a 60 minutes pre-incubation time both with non-differentiated and differentiated cells.

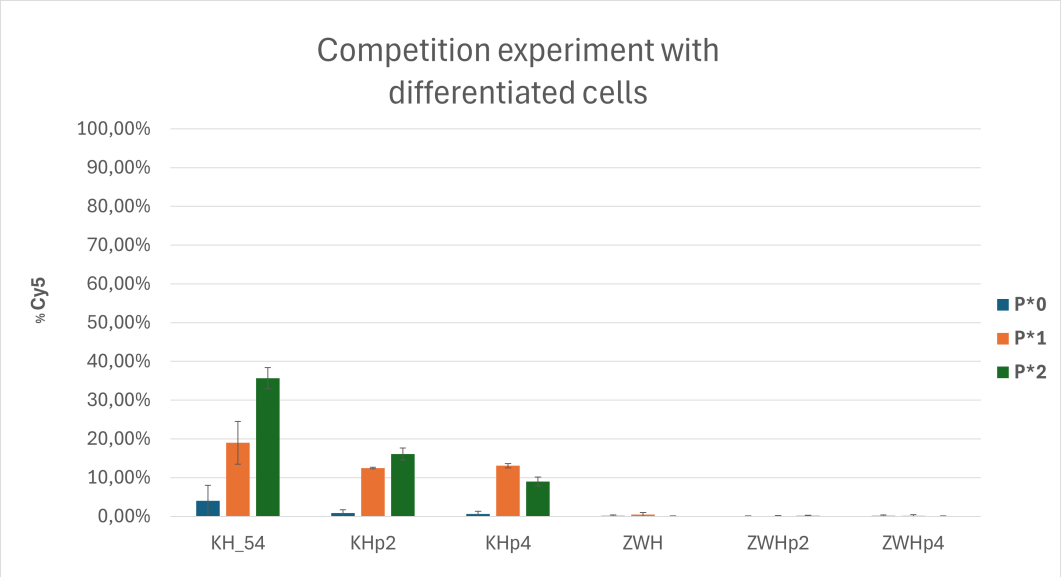

Figure 3.18: Competition experiment done with differentiated C2C12. The pre-incubation time was of 30 minutes and the NPs were left to incubate overnight. In this case the peptide was diluted in milliQ water.

The competition experiment done with non-differentiated cells (**Figure 3.19**) gave results that were more similar to the ones obtained with the uptake experiments, except for KHp2 that was oddly low. It stayed around 10% in all three uptakes. Leaving it aside, the uptakes were higher and they were not in contrast with the previous results: KH_{54} was between 70% and 80%, while the others were around 40%-60%. Looking at the three uptakes of KH_{54}, KHp2, KHp4 and ZWHp2 is possible to notice a slight lowering, but it is not significant and statistically valid. Additionally, it cannot be observed in ZWHp4 and the uptake of KH_{54} shouldn't actually be influenced. Regarding the experiment with the differentiated C2C12

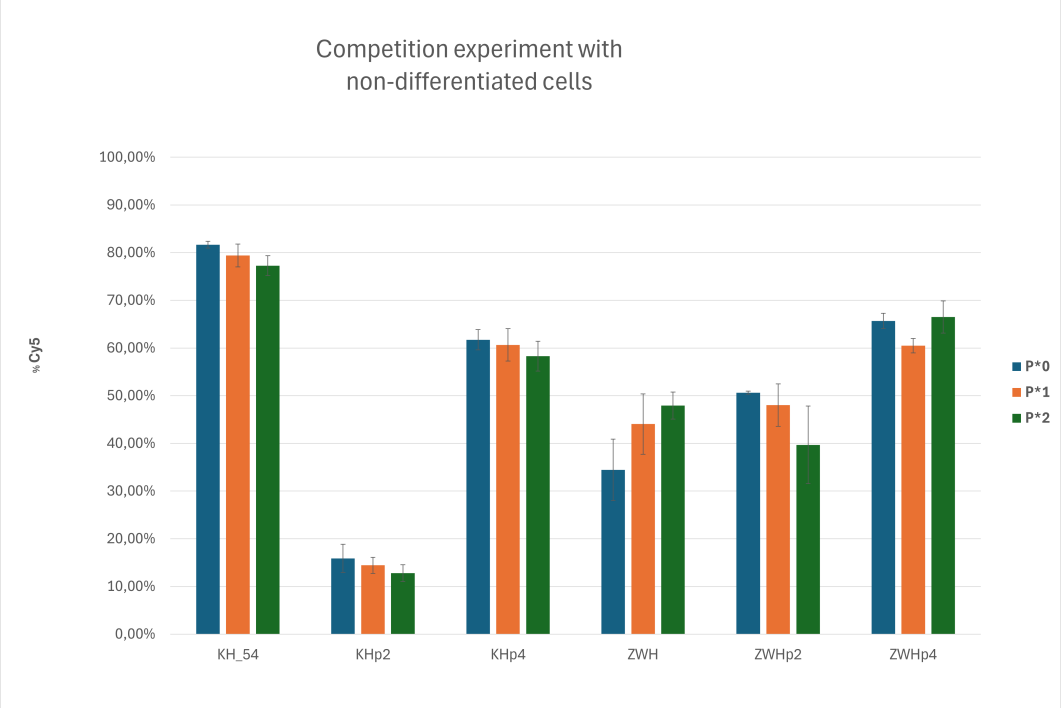

Figure 3.19: Competition experiment done with non-differentiated cells. The pre-incubation time was of 60 minutes and the following incubation time was 6 hours.

(**Figure 3.20**), we had better results as for the uptakes values for the non zwitterionic NPs. The uptakes are still lower than the ones shown previously, as they are around 30%, but higher than the previous competition experiment (**Figure 3.18**). KH_{54}, KHp2 and KHp4 don't show any pattern.Furthermore, the zwitterionic NPs did not apparently enter the cells, as their uptakes are very low.
Anyway, we calculated the difference between the three uptakes to see if we could find a pattern, especially where there appeared to be in the graphics, but the results were inconclusive.

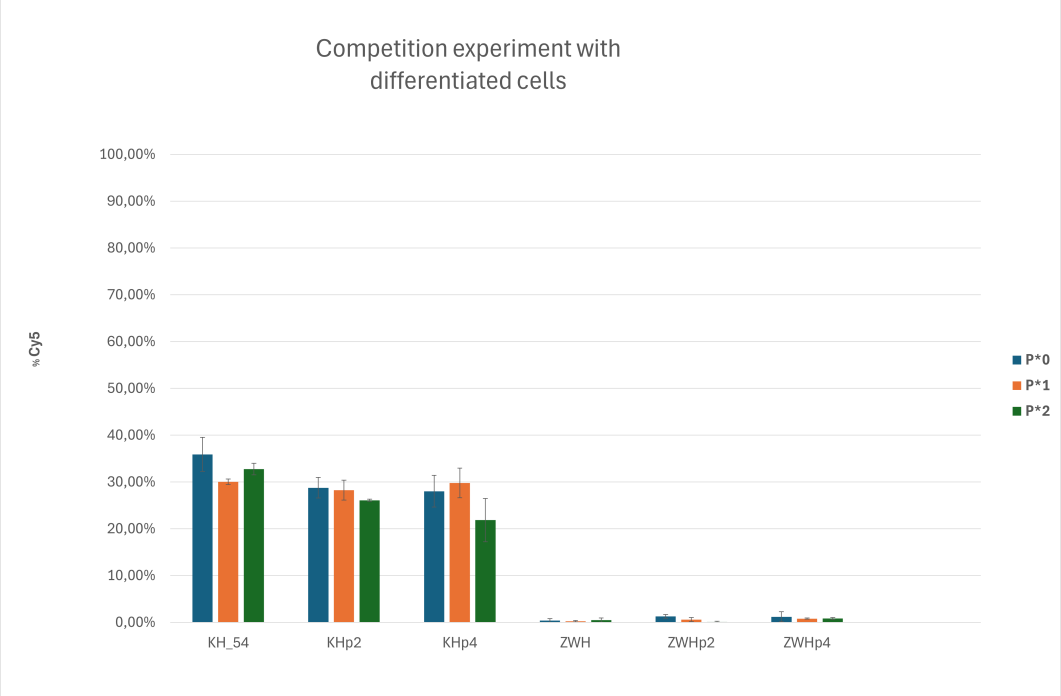

Figure 3.20: Competition experiment done with differentiated C2C12. The pre-incubation time was of 60 minutes and the NPs were left to incubate overnight.

The competition experiments required an high number of cells and were quite demanding to run, especially with the differentiated cells that are more delicate to work with. We carried out the experiments twice and every sample was in triplicate, but for future developments, it would be better to repeat them.
Anyway, given our results, we can conclude that the targeting peptides were not working as we wanted,specifically binding with the integrin $\alpha_7\beta_1$. Considering what we deduced from the **section 3.4**, we were sure that the peptides were encapsulated, so consequently we thought that the next step should be to investigate and to improve their exposition. If the peptides were exposed enough, it would be more easy for them to bind with the target.

3.6 Synthesis and characterization of OM-pBAEs-DBCO NPs

The NPs we synthesized until now have the targeting peptides capped to the polymers at the end of the polymeric chain . A consequence of this could be a poor exposition of the peptides. One possible strategy to improve this aspect could be to change the position of the peptides and have them attached laterally to the polymers. A way to do so is to use DBCO-NH (**Figure 3.21**). GEMAT group had already synthesized a OM-pBAE polymer with DBCO-NH (C6-DBCO) that we used in this last part of the project. DBCO is a class of reagents and contains a very reactive group. It can

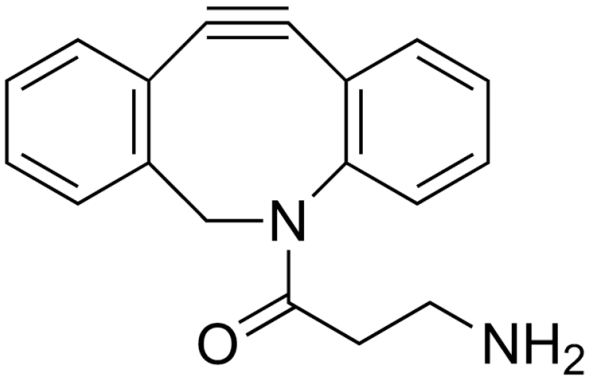

Figure 3.21: Chemical structure of DBCO-NH ([34]).

react with the azide group linked to other molecules via copper-free click chemistry, which can be run in aqueous buffer [35]. Click chemistry reactions are defined as selective, high yielding, and having good reaction kinetics reactions. In particular, the reaction between DBCO-NH and the azide group is a cycloaddition and it is part of a group called orthogonal reactions since the components of the click reaction are inert to the possible surrounding species [36].

As described in **section 2.3**, we synthesized the NPs and we analyzed them with the NTA and the DLS (**Figure 3.21**).

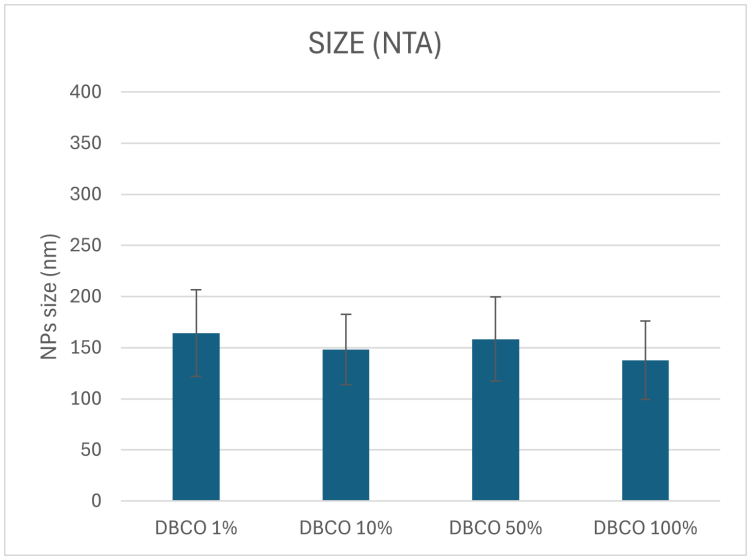

(A)

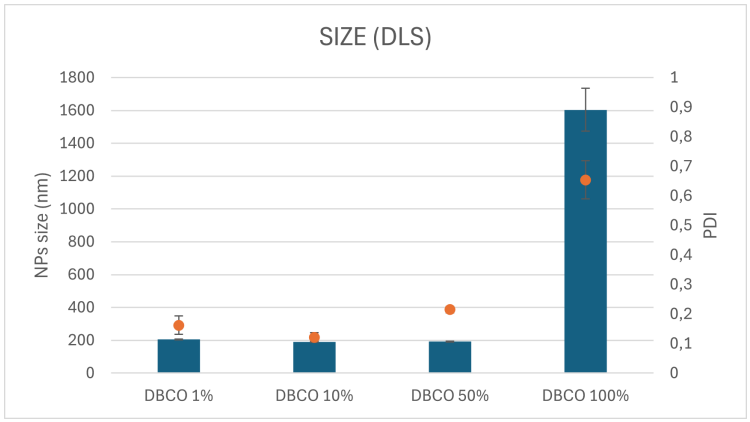

(B)

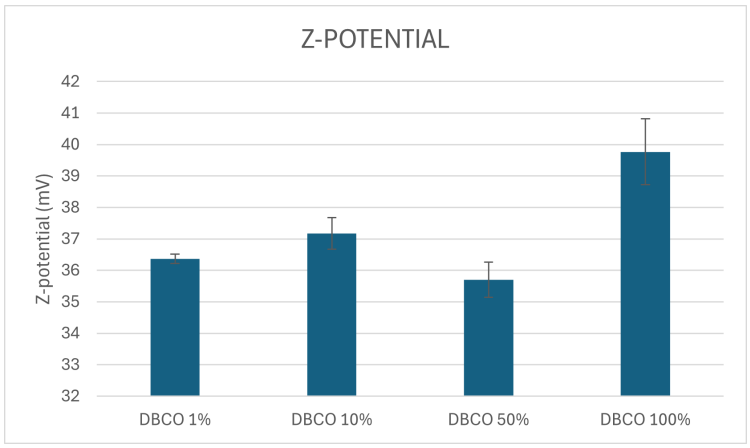

(C)

Figure 3.22: Characterization of the size of NPs with DBCO by NTA (A) and by DLS (B). Characterization of Z-potential of NPs by DLS (C). In (A) it is also shown the PDI (red dots).

Observing the results from the NTA (**Figure 3.22 (A)**), the size of the NPs, around 150 nm, is quite good for all the samples. However, the results given by the DLS (**Figure 3.22 (B)**)reveal that the NP $DBCO_{100\%}$ is too big: it is around 1600 nm. Its PDI is too high as well, showing that probably aggregates of different sizes were formed during the synthesis. It may be that having this high amount of C6-K-DBCO doesn't allow the formation of a proper NP. The discrepancy between the results obtained by DLS and NTA arises from the fundamental differences in their measurement principles. DLS is highly sensitive to larger particles and this affects the final result, increasing the average particle size. In contrast, NTA. is more accurate in sizing smaller particles, but it can be less sensitive with larger ones [37]. If the aggregates are just a few or unstable, it's possible that it did not detect them, but that does not mean they are not present in the sample. As concerns the other NPs, $DBCO_{1\%}$,$DBCO_{10\%}$ and $DBCO_{50\%}$, they present an adequate size, around 200 nm. Their PDIs are between 0,1 and 0,2, which proves that the samples are monodisperse. The PDI of $DBCO_{50\%}$ is slightly higher comparing to the other two samples, so probably we are getting closer to the maximum quantity of C6-K-DBCO to have a NP with the characteristics we want. Regarding the Z-potential, excluding $DBCO_{100\%}$, it goes between 35 and 38, which is higher than the values found for the other type of NPs. The Z-potential of $DBCO_{100\%}$ is not really relevant, given its size.

3.7 Uptakes with OM-pBAEs-DBCO NPs

As very last experiment, we decided to try doing an uptake with OM-pBAEs-DBCO NPs. It is important to notice that this experiment was repeated only once with triplicate for each sample, due to a lack of the polymer with DBCO. We tried to synthesize it, but we couldn't have proper results, as the DBCO did not seem to be included in the polymeric structure. For this reason, we chose to run the uptake only with the differentiated cells, as they are the real target for our research. Once characterized the NPs, we selected the NPs $DBCO_{1\%}$ and $DBCO_{10\%}$. Hence, we added to the NPs the peptide with the azide group in the same quantity calculated in the competition experiments for the free peptide. The protocol followed is described in the **section 2.3**. The uptake was done with the NPs cited above with and without the addition of the peptide (**Figure 3.23**) and the incubation time chosen was of 4 hours. Observing the results, it is possible to notice that the uptakes, between

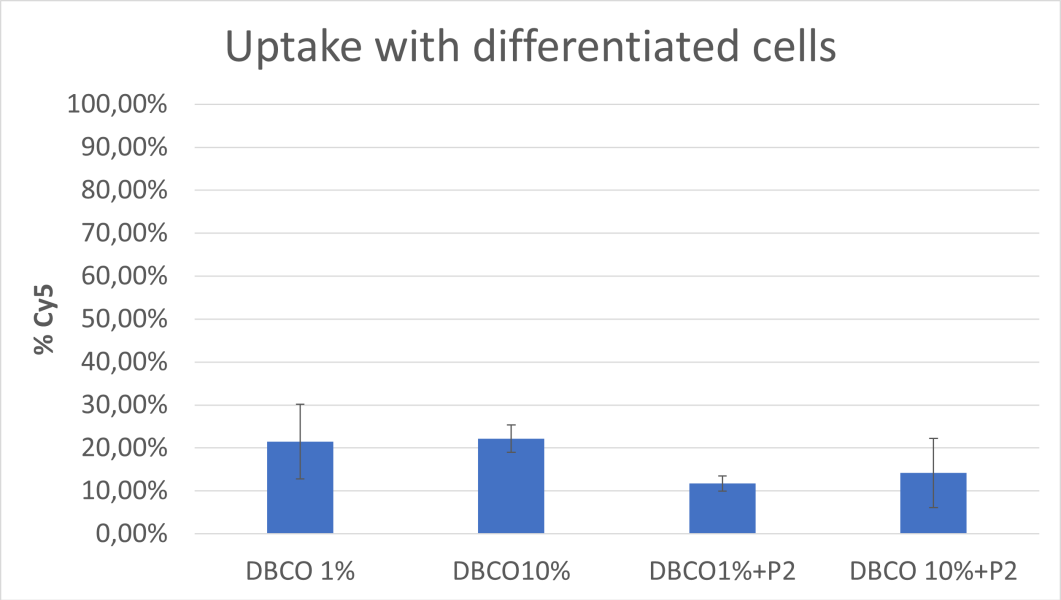

Figure 3.23: Uptake done with OM-pBAEs-DBCO NPs. Differentiated cells were used and the incubation time was of 4 hours.

10% and 20%, are not very high, but not as low as other uptakes we had with the differentiated cells and the incubation time is only 4 hours. The uptakes with the NPs with the targeting peptide are slightly lower than the others, so the results are not what we expected. However, this new strategy could be a solution to optimize the results. This uptake was repeated only once, as already mentioned, so it it fundamental to try again, maybe with different quantity of the targeting peptide and different timing of incubation.

Chapter 4

Conclusion

The findings from the experiments conducted in this Master's thesis support the following conclusions:

- The presence of $\alpha_7\beta_1$ and the expression of Desmin in our model cell C2C12 integrin was confirmed with confocal immunofluorescence: In both cases, it was possible to notice the difference of expression and location between the non-differentiated and differentiated cells;
- The presence of $\alpha_7\beta_1$ and the expression of Desmin in our model cell C2C12 integrin was confirmed with confocal immunofluorescence: In both cases, it was possible to notice the difference of expression and location between the non-differentiated and differentiated cells;
- The synthesis and characterization of the NPs composed by OM-pBAEs and the zwitterionic polymer were successful and gave suitable results for the following steps;
- It was demonstrated that uptake is more difficult and slower with differentiated cells and that, always with these cells, the targeting peptides don't guarantee a higher uptake;
- OM-pBAEs NPs allow a quite high uptake, while the zwitterionic NPs a lower one;
- The study of the colocalization of the PGFP and the targeting peptides showed positive results, as both were encapsulated in the NPs;
- Performing a competition experiment between the NPs and the free peptide, we confirmed that the targeting peptides were not specifically binding with $\alpha_7\beta_1$ integrin;
- The synthesis and characterization of OM-pBAEs-DBCO NPs helped us to have a first selection of possible DBCO NPs composition, ruling out $DBCO_{100\%}$, but both have to be studied more, together with the uptakes with these NPs.

Chapter 5

Future Perspectives

Regarding the future steps to take, the first path to follow could be to deepen the analysis regarding the OM-pBAEs-DBCO NPs. In this project, we synthesized NPs only trying with four different percentage of OM-pBAEs-DBCO polymer, but it is important to optimize the best quantity. It is also essential to understand the right incubation time when adding the new compound while synthesizing the NPs. After these first fundamental steps, it will be possible to investigate and compare the different NPs.
Moreover, another possible path to investigate more is the zwitterionic polymer, given its interesting features. What could be studied is a different way to incorporate it to the OM-pBAEs polymers.
Recently the research group of Palacio et al. has published an article where they show a new strategy to specifically target muscle cells [38]. They describe a gold NP conjugated to an aptamer, a class of nucleic acid with a high binding affinity to the target molecule. It targets $\alpha_7\beta_1$ integrin, too. In their work they deliver another miR, but it is possible to conjugate different types of oligonucleotides. This work is interesting because their NP seems to work successfully and they are using another method to target muscle cells, which we could try to integrate in our NPs. There are, indeed, many possible strategies that can be followed, but the use of OM-pBAEs definitely gives many advantages thanks to their features, their biocompatibility and biodegradability.

Bibliography

[1] D. Duan. "Systemic AAV Micro-dystrophin Gene Therapy for Duchenne Muscular Dystrophy". In: *Molecular Therapy* 26,10 (Oct. 2018), pp. 2337–2356. DOI: https://doi.org/10.1016/j.ymthe.2018.07.011 (cit. on p. 1).

[2] D. Duan et al. "Duchenne muscular dystrophy". In: *Nature Reviews Disease Primers* 7, 13 (Feb. 2021). DOI: https://doi.org/10.1038/s41572-021-00248-3 (cit. on p. 1).

[3] J. Deng et al. "Drug development progress in duchenne muscular dystrophy". In: *Frontiers in Pharmacology* 13 950651 (July 2022). DOI: https://doi.org/10.3389/fphar.2022.950651 (cit. on pp. 1, 2, 4, 6).

[4] Gao et al. "The Dystrophin Complex: Structure, Function, and Implications for Therapy". In: *Comprehensive Physiology* 5,3 (2015), pp. 1223–1239. DOI: https://doi.org/10.1002/cphy.c140048 (cit. on p. 1).

[5] Sheridan et al. "Duchenne muscular dystrophy awaits gene therapy". In: *Nature Biotechnology* 37 (Apr. 2019), pp. 333–334. DOI: https://doi.org/10.1038/s41587-019-0101-7 (cit. on pp. 2, 6).

[6] Eppie M. et al. "Duchenne Muscular Dystrophy". In: *Journal of Paediatrics and Child Health* 51,8 (Aug. 2015), pp. 759–764. DOI: https://doi.org/10.1111/jpc.12868 (cit. on pp. 3, 4).

[7] Wenger et al. "The Pediatric and Adolescent Hip: Essentials and Evidence". In: *Journal of pediatric orthopedics,* 40, 7 (2020), e667. DOI: https://doi.org/10.1097/BPO.0000000000001448 (cit. on p. 3).

[8] Elangkovan N. et al. "Gene Therapy for Duchenne Muscular Dystrophy". In: *Journal of Neuromuscular Disease* 8, s2 (2021), S303–S316. DOI: https://doi.org/10.3233/JND-210678 (cit. on p. 6).

[9] Aranega et al. "MiRNAs and Muscle Regeneration: Therapeutic Targets in Duchenne Muscular Dystrophy". In: *International Journal of Molecular Sciences* 22,8 (Apr. 2021), p. 4238. DOI: https://doi.org/10.3390/ijms22084236 (cit. on pp. 6, 7).

[10] Rodriguez-Outeriño et al. "miR-106b is a novel target to promote muscle regeneration and restore satellite stem cell function in injured Duchenne dystrophic muscle". In: *Molecular Therapy-Nucleic Acids* 29 (Sept. 2022), pp. 769–786. DOI: https://doi.org/10.1016/j.omtn.2022.08.025 (cit. on p. 8).

[11] *Ambion™ mirVana™ miRNA Inhibitor*. Cited in 6 may 2025. URL: https://www.fishersci.dk/shop/products/i-mir-i-vana-mirna-inhibitor-18/13416706 (cit. on p. 8).

[12] Fornaguera C. et al. "Unraveling polymeric nanoparticles cell uptake pathways: Two decades working to understand nanoparticles journey to improve gene therapy". In: *In Turksen K(Ed.), Cell biology and translational medicine* 9 (2020), pp. 117–138. DOI: https://doi.org/10.1007/5584_2019_467 (cit. on pp. 8–10, 14).

[13] Vocabulary. British Standards Institution. *Nanoparticles*. Cited in 6 may 2025. URL: https://knowledge.bsigroup.com/products/nanoparticles-vocabulary (cit. on p. 9).

[14] Awan et al. "Nanoparticles' classification, synthesis, characterization and applications—A review". In: *Characterization and Application of Nanomaterials* 8, 1 (Nov. 2024), p. 8899. DOI: https://doi.org/10.24294/can8899 (cit. on p. 9).

[15] Jeevanandam et al. "Review on nanoparticles and nanostructured materials: history, sources, toxicity and regulations". In: *Beilstein Journal of Nanotechnology* 9 (Apr. 2018), pp. 1050–1074. DOI: https://doi.org/10.3762/bjnano.9.98 (cit. on p. 9).

[16] Barhoum A. et al. "Review on Natural, Incidental, Bioinspired, and Engineered Nanomaterials: History, Definitions, Classifications, Synthesis, Properties, Market, Toxicities, Risks, and Regulations". In: *Nanomaterials* 12,2 (2022), p. 177. DOI: https://doi.org/10.3390/nano12020177 (cit. on p. 9).

[17] Eker et al. "A Comprehensive Review of Nanoparticles: From Classification to Application and Toxicity". In: *Molecules* 9, 15 (July 2024), p. 3482. DOI: https://doi.org/10.3390/molecules29153482 (cit. on pp. 10, 11).

[18] Segovia N. et al. "Oligopeptide-terminated poly(-amino ester)s for highly efficient gene delivery and intracellular localization". In: *Acta Biomaterialia* (2014). DOI: http://dx.doi.org/10.1016/j.actbio.2013.12.054 (cit. on pp. 11, 12, 14).

[19] Fornaguera C. et al. "mRNA Delivery System for Targeting Antigen-Presenting Cells In Vivo". In: *Advanced Healthcare Materials* 7 (2018). DOI: https://doi.org/10.1002/adhm.201800335 (cit. on pp. 12, 14).

[20] Lynn et al. "egradable poly(-amino esters): synthesis, characterization, and self-assembly with plasmid DNA". In: *Journal of the American Chemical Society* 122, 44 (2000). DOI: https://doi.org/10.1021/ja0015388 (cit. on p. 12).

[21] Magaña Rodriguez et al. "Nucleic acid-loaded poly(beta-aminoester) nanoparticles for cancer nano-immuno therapeutics: the good, the bad, and the future". In: *Drug Delivery and Translational Research* 14 (May 2024), pp. 3477–3493. DOI: https://doi.org/10.1007/s13346-024-01585-y (cit. on pp. 12, 13).

[22] National Center for Biotechnology Information (2025). *PubChem Compound Summary for CID 5962, Lysine*. Cited in 13 May 2025. URL: https://pubchem.ncbi.nlm.nih.gov/compound/Lysine (cit. on p. 13).

[23] National Center for Biotechnology Information (2025). *PubChem Compound Summary for CID 6322, Arginine*. Cited in 13 May 2025. URL: https://pubchem.ncbi.nlm.nih.gov/compound/Arginine (cit. on p. 13).

[24] National Center for Biotechnology Information (2025). *PubChem Compound Summary for CID 6274, Histidine*. Cited in 13 May 2025. URL: https://pubchem.ncbi.nlm.nih.gov/compound/Histidine (cit. on p. 13).

[25] Dosta et al. "Surface charge tunability as a powerful strategy to control electrostatic interaction for high efficiency silencing, using tailored oligopeptide-modified poly(beta-amino ester)s (PBAEs)". In: *Acta Biomaterialia* 20 (July 2015), pp. 82–93. DOI: https://doi.org/10.1016/j.actbio.2015.03.029 (cit. on p. 14).

[26] Navalon-Lopez et al. "Unravelling the role of individual components in pBAE/polynucleotide polyplexes in the synthesis of tailored carriers for specific applications: on the road to rational formulations". In: *Nanoscale Advances* 5.6 (2023), pp. 1611–1623. DOI: https://doi.org/10.1039/D2NA00800A (cit. on pp. 14, 29).

[27] M. Rodriguez et al. "Nucleic acid-loaded poly(beta-aminoester) nanoparticles for cancer nano-immuno therapeutics: the good, the bad, and the future". In: *Drug Delivery and Translational Research* 14 (2024), pp. 3477–3493. DOI: https://doi.org/10.1007/s13346-024-01585-y (cit. on pp. 14, 29, 32).

[28] García-Fernández et al. "Stealth mRNA nanovaccines to control lymph node trafficking". In: *Journal of Controlled Release* 374 (Oct. 2024), pp. 325–336. DOI: https://doi.org/10.1016/j.jconrel.2024.08.018 (cit. on p. 15).

[29] Weinmann et al. "Identification of a myotropic AAV by massively parallel in vivo evaluation of barcoded capsid variants". In: *Nature communications* 11 (Oct. 2020). DOI: https://doi.org/10.1038/s41467-020-19230-w (cit. on pp. 16, 36).

[30] *C2C12*. Cited in 10 february 2025. URL: https://www.atcc.org/products/crl1772#detailed-product-information (cit. on p. 23).

[31] M. J. McClure et al. "Role of Integrin 7 1 Signaling in Myoblast Differentiation on Aligned Polydioxanone Scaffolds". In: *Acta Biomaterialia* 39 (2016), pp. 44–54. DOI: https://doi.org/10.1016/j.actbio.2016.04.046 (cit. on p. 27).

[32] C. Hakibilen et al. "Desmin Modulates Muscle Cell Adhesion and Migration". In: *Frontiers in Cell and Developmental Biology* 10 (Mar. 2022). DOI: https://doi.org/10.3389/fcell.2022.783724 (cit. on p. 28).

[33] Wang et al. "Glioma and microenvironment dual targeted nanocarrier for improved antiglioblastoma efficacy". In: *Drug delivery* 24,1 (2017), pp. 1401–1409. DOI: https://doi.org/10.1080/10717544.2017.1378940 (cit. on p. 45).

[34] *Dibenzocyclooctyne-amine*. Cited in 3 april 2025. URL: https://www.sigmaaldrich.com/ES/es/product/aldrich/761540?srsltid=AfmBOoprh821Z5VBoKCSorozP2H6ulmVQKSBQV3LPORL9lftSnkdGupw (cit. on p. 52).

[35] *DBCO*. Cited in 7 april 2025. URL: https://broadpharm.com/product-categories/click-chemistry-reagents/dbco (cit. on p. 52).

[36] C.O. Kappe et al. "Cu-free click cycloaddition reactions in chemical biology". In: *Chemical Society Reviews* 39,4 (2010), pp. 1280–1290. DOI: http://dx.doi.org/10.1039/B901973C (cit. on p. 52).

[37] Filipe et al. "Critical Evaluation of Nanoparticle Tracking Analysis (NTA) by NanoSight for the Measurement of Nanoparticles and Protein Aggregates". In: *Pharmaceutical Research* 27,5 (May 2010), pp. 796–810. DOI: https://doi.org/10.1007/s11095-010-0073-2 (cit. on p. 54).

[38] Milozzi F. et al. "Aptamer-conjugated gold nanoparticles enable oligonucleotide delivery into muscle stem cells to promote regeneration of dystrophic muscles". In: *Nature Communications* 16, 1 (Jan. 2025), p. 577. DOI: https://doi.org/10.1038/s41467-024-55223-9 (cit. on p. 57).

Dedications

I would like first to express my sincere gratitude to Prof. Valentina Alice Cauda who allowed me to take part in this incredible experience in Barcelona and for her constant availability and support.
I am also deeply grateful to Prof. Marta Guerra Rebollo for her invaluable guidance, support, and encouragement throughout the development of this thesis. Her insightful feedback and constant availability were fundamental for the outcome of this project.
I would like to thank the entire team of professors and PhD students at GEMAT that supported me, not only in my research, throughout my stay.